

DOI: 10.1159/000512685

Received: 6/24/2020

Accepted: 10/29/2020

Published(online): 10/30/2020

-----  
CORTISOL CIRCADIAN RHYTHM AND INSULIN RESISTANCE IN MUSCLE: EFFECT OF DOSING AND TIMING OF  
HYDROCORTISONE EXPOSURE ON INSULIN SENSITIVITY IN SYNCHRONIZED MUSCLE CELLS.

Negri M. Pivonello C. Simeoli C. Di Gennaro G. Venneri M.A. Sciarra F. Ferrigno R. de  
Angelis C. Sbardella E. De Martino M.C. Colao A. Isidori A.M. Pivonello R.

-----  
ISSN: 0028-3835 (Print), eISSN: 1423-0194 (Online)

<https://www.karger.com/NEN>

Neuroendocrinology  
-----

Disclaimer:

Accepted, unedited article not yet assigned to an issue. The statements, opinions and data contained in this publication are solely those of the individual authors and contributors and not of the publisher and the editor(s). The publisher and the editor(s) disclaim responsibility for any injury to persons or property resulting from any ideas, methods, instructions or products referred to in the content.

Copyright:

All rights reserved. No part of this publication may be translated into other languages, reproduced or utilized in any form or by any means, electronic or mechanical, including photocopying, recording, microcopying, or by any information storage and retrieval system, without permission in writing from the publisher.

© 2020 S. Karger AG, Basel  
-----

Accepted manuscript

# **CORTISOL CIRCADIAN RHYTHM AND INSULIN RESISTANCE IN MUSCLE: EFFECT OF DOSING AND TIMING OF HYDROCORTISONE EXPOSURE ON INSULIN SENSITIVITY IN SYNCHRONIZED MUSCLE CELLS.**

Mariarosaria Negri<sup>a\*</sup>, Claudia Pivonello<sup>a\*</sup>, Chiara Simeoli<sup>a</sup>, Gilda Di Gennaro<sup>a</sup>, Mary Anna Venneri<sup>b</sup>, Francesca Sciarra<sup>b</sup>, Rosario Ferrigno<sup>a</sup>, Cristina de Angelis<sup>a</sup>, Emilia Sbardella<sup>b</sup>, Maria Cristina De Martino<sup>a</sup>, Annamaria Colao<sup>a,c</sup>, Andrea Isidori<sup>b</sup>, Rosario Pivonello<sup>a,c</sup>.

<sup>a</sup>Dipartimento di Medicina Clinica e Chirurgia, Sezione di Endocrinologia, Università Federico II di Napoli, Naples, Italy;

<sup>b</sup>Department of Experimental Medicine, Sapienza University of Rome, Rome, Italy;

<sup>c</sup>UNESCO Chair on Health Education and Sustainable Development, Federico II University, Naples, Italy.

\*Both authors equally contributed to the work.

Short title: hydrocortisone circadian levels and insulin resistance

Correspondence:

Rosario Pivonello, MD PhD

Dipartimento di Medicina Clinica e Chirurgia

Università “Federico II” di Napoli,

Via Sergio Pansini, 5

80131 Naples, Italy

Tel: +39 0817464983

Fax: +39 0817464983

Email: [rosario.pivonello@unina.it](mailto:rosario.pivonello@unina.it)

Number of Tables: 3; 3 in supplementary data

Number of Figures: 9; 1 in supplementary data

Word count: 6405

Keywords: cortisol circadian rhythm, clock genes, adrenal insufficiency, insulin resistance

## ABSTRACT

**Introduction/Aim:** Circadian rhythm disruption is emerging as a risk factor for metabolic disorders and particularly, alterations in clock genes circadian expression have been shown to influence insulin sensitivity. Recently, the reciprocal interplay between the circadian clock machinery and HPA axis has been largely demonstrated: the circadian clock may control the physiological circadian endogenous glucocorticoids secretion and action; glucocorticoids, in turn, are potent regulator of the circadian clock and their inappropriate replacement has been associated with metabolic impairment. The aim of the current study was to investigate *in vitro* the interaction between the timing-of-the-day exposure to different hydrocortisone (HC) concentrations on muscle insulin sensitivity.

**Methods:** Serum-shock synchronized mouse skeletal muscle C2C12 cells were exposed to different HC concentrations recapitulating the circulating daily physiological cortisol profile (standard cortisol profile), the circulating daily cortisol profile that reached in adrenal insufficient (AI) patients treated with once-daily MR-HC (flat cortisol profile) and treated with thrice-daily of conventional IR-HC (steep cortisol profile). The 24 hrs spontaneous oscillation of the clock genes in synchronized C2C12 cells was used to align the timing for *in vitro* HC exposure (*Bmal1* acrophase, midphase and bathyphase) with the reference times of cortisol peaks in AI treated with IR-HC (8 am, 1 pm, 6 pm). A panel of 84 insulin sensitivity related genes and intracellular insulin signaling proteins were analyzed by RT-qPCR and western blot, respectively.

**Results:** Only the steep profile, characterized by a higher HC exposure during *Bmal1* bathyphase, produced significant downregulation in 21 insulin sensitivity-related genes. Among these, *Insr*, *Irs1*, *Irs2*, *Pi3kca* and *Adipor2* were downregulated when compared the flat to the standard or steep profile. Reduced intracellular IRS1 Tyr608, AKT Ser473, AMPK Thr172 and ACC Ser79 phosphorylations were also observed.

**Conclusions:** The current study demonstrated that is late-in-the-day cortisol exposure that modulates insulin sensitivity-related genes expression and intracellular insulin signaling in skeletal muscle cells.

## INTRODUCTION

In humans, the endogenous circadian clock regulates a great number of daily physiological and behavioral processes [1,2]. The master clock, residing in the suprachiasmatic nuclei (SCN) of the hypothalamus, receives information from external and internal inputs, including light-dark and sleep-wake cycles, hunger-feeding-satiety circle, temperature shift, and stressors, and activates responses aimed at synchronizing the peripheral clocks with exogenous and endogenous inputs [3,4]. Clock genes and proteins oscillate at the single-cell level through finely regulated transcriptional and translational feedback loops [5]. According to the “canonical model”, two main clock proteins, which function as gene activators, BMAL1 (brain and muscle aryl hydrocarbon receptor nuclear translocator (ARNT)-like protein 1) and CLOCK, after forming the complex BMAL1/CLOCK by heterodimerization in the cytoplasm, translocate into the nucleus to induce the gene expression of the clock proteins, PERIOD (PER1/2/3) and CRYPTOCROME (CRY1/2) [6]. PER and CRY, which function as gene repressors, after forming the complex PER/CRY by heterodimerization in the cytoplasm, translocate into the nucleus to repress gene expression, and consequently activity, of BMAL1/CLOCK complex, which is also able to repress PER/CRY protein expression, and consequently activity, by the activation of a proteasome-mediated pathway [6]. Clock genes and proteins rhythmically communicate throughout the day to compose the circadian clock machinery, which displays a specific daily rhythm: BMAL1/CLOCK complex accumulates in the cytoplasm at the beginning of a subjective day, while PER/CRY complex accumulates in the cytoplasm at the beginning of a subjective night [7,8].

An intricate interplay between the circadian clock and the hypothalamus-pituitary-adrenal (HPA) axis has been demonstrated in several *in vitro* and *in vivo* studies on animal and human models [9–21]. In particular, several evidences have demonstrated that the circadian clock may control the physiological circadian endogenous glucocorticoids (GCs) secretion, in *in vivo* animal [9–13] and human [14] models, and the daily physiological response to the endogenous GCs, through the activation of different mechanisms inhibiting GC receptor function, in *in vitro* animal [15] and human [16,17] models. On the other hand, GCs have been found to synchronize the expression of the circadian clock in *in vitro* animal [18] and human [19] cell models and in *in vivo* animal models [20,21]. Moreover, it is well established that chronic GC excess in animals and humans is associated with insulin resistance [22-27] mainly due to the impairment of insulin receptor expression and signaling in skeletal muscle as largely demonstrated in *in vitro* human models [22,23] and *in vivo* animals [22,24] and human models [25-27]. The peripheral circadian clock has been documented to regulate a series of functions related to various systems, including metabolism,

as demonstrated by the evidence that the circadian rhythm disruption has been associated with metabolic disorders in *in vivo* studies on either animal or human models [28-34]. Indeed, mouse models with disruption of circadian clock [28-31] developed obesity and metabolic disorders, whereas human models with a genetic variant of a clock machinery component [32] or a misalignment of circadian clock machinery rhythm [33] developed impairment of glucose metabolism, and/or insulin sensitivity in skeletal muscle, and interestingly, in a model of an obese population, adipose tissue cell variability of circadian clock was associated with visceral obesity and metabolic syndrome [34]. Furthermore, recent studies showed that skeletal muscle genes follow a circadian expression as well as myogenesis, fiber-type shifts and mitochondrial respiration [35].

The cohort of the studies demonstrating the interplay between the circadian clock and the HPA axis from one side, and the cohort of the studies demonstrating a connection between the circadian clock disruption and the disorders of metabolism, especially impairment of glucose metabolism and insulin sensitivity, from the other side, suggested that the insulin resistance and consequent metabolic syndrome induced by the disruption of the circadian clock might be mediated by the disruption, especially in terms of rhythm loss, of the HPA axis, that in turn might induce an impairment of metabolic state through the disruption of the circadian clock, especially in terms of rhythm loss.

In humans, the HPA axis disorders, associated with GC excess or deficiency, mainly include hypercortisolism or Cushing's syndrome (CS), characterized by cortisol excess in the endogenous form and GCs excess in the exogenous form, and hypocortisolism or adrenal insufficiency (AI), characterized by cortisol deficiency [38,40]. The exposure to cortisol excess and deficiency, which are associated with disruption of the physiological circadian cortisol rhythm, negatively affects morbidity and mortality [37,41-43]. Indeed, CS is associated with increased mortality and several comorbidities, including metabolic syndrome, generally characterized by insulin resistance and glucose intolerance or diabetes [37]. Similarly, AI, requiring lifelong replacement therapy with GCs, generally represented by hydrocortisone (HC), is also associated with increased mortality and several comorbidities, which however appear to be related to inadequate GC replacement [40]. Indeed, GC dose and timing adjustments are the main challenges to avoid the imbalance between overtreatment and undertreatment, and to replicate the physiological cortisol circadian rhythm. Specifically, the overall cortisol exposure, consequent to the daily doses of conventional GC treatments routinely used in the majority of patients, appears to be higher than that observed during the normal daily cortisol production [42]. The GC overexposure has been found to be associated with an increased mortality [41,42] and an increased risk of developing the typical CS

comorbidities, including metabolic syndrome [43,44], characterized by insulin resistance and glucose intolerance or diabetes [45,46]. More recently, patients treated with conventional GC formulations, especially immediate-release hydrocortisone (IR-HC), administered twice or thrice daily, and therefore exposed to non-physiological pattern of circadian cortisol profile, but to daytime cortisol peaks and troughs, and particularly to the elevated diurnal evening cortisol levels, have shown more deleterious effects, especially on metabolic state, when compared with patients treated with the novel formulation of modified released hydrocortisone (MR-HC) [47-55]. Indeed, a novel MR-HC formulation, based on an immediate release coating, together with an extended release core, orally administered once daily in the morning, was found to better mimic the circadian cortisol profile, by reducing diurnal cortisol peaks and troughs, and particularly the diurnal evening cortisol overexposure, with notable improvement of metabolic state [47-55] suggesting that the achievement of the optimal GC timing, beyond dosing, is relevant for the maintenance of a better metabolic profile.

However, the role of the disruption of circadian GC rhythm and the consequent daily profile, as well as the effects of non-physiological cortisol exposure in different phases or time-points of cell circadian rhythm on the molecular regulation of insulin sensitivity has never been investigated in the skeletal muscle.

To this purpose, the current study aims at investigating the molecular effects of physiological and non-physiological exposure to HC, the main exogenous GC, along various phases of the cell circadian rhythm, on insulin sensitivity in an experimental model of mouse skeletal muscle cell.

## **MATERIALS AND METHODS**

### **Study design**

The current *in vitro* study aims at exploring the effects of physiological and non-physiological HC concentrations, administered in different time-points of circadian rhythm, on skeletal muscle insulin sensitivity. The model used for the study is a mouse skeletal muscle cell line, the C2C12 myocytes appropriately obtained by the differentiation of respective myoblasts; this model is usually assessed for *in vitro* studies on cell proliferation, but also on glucose uptake and utilization, glycogen synthesis, insulin response, mitochondrial activity, protein synthesis, glucose and fatty acids oxidation, as well as skeletal muscle contractile activity. The study protocol initially required C2C12 myocytes synchronization, a process by which *in vitro* cells can assume an autonomous and

self-sustained circadian expression of components of circadian clock. The synchronization has been performed by a serum shock protocol and has been verified by following the oscillation of clock genes expression every 4 hrs for a consecutive 24 hrs interval of time, in order to set the time-points of exposure to HC. Although a mouse cell model, C2C12, was used for the current study, HC, and not corticosterone, was administered for the *in vitro* experiments to better mimic the human condition, without affecting the experimental results having HC and corticosterone the same binding affinity for GR [56,57]. The main experiment was based on the exposure of the C2C12 myocytes to different HC concentrations in the different time-points of the circadian rhythm of the synchronized cells and to measure the effects on insulin sensitivity. The aspects of insulin sensitivity evaluated during the experiments were: 1) a general analysis of insulin sensitivity, performed by the evaluation of gene expression profile through RT-qPCR insulin resistant-related array investigating the simultaneous expression levels of 84 key genes involved in the cell mechanisms regulating insulin sensitivity, and consequently involved in the development of insulin resistance; 2) a specific analysis of insulin receptor signaling, the main determinant of insulin sensitivity, performed by the evaluation of gene expression profile through RT-qPCR; and 3) a specific analysis of crucial intracellular mechanisms associated with insulin sensitivity, performed by the evaluation of protein expression through western blot. On the basis of the results obtained at genomic level, the mechanisms investigated through western blot included not only the pathways strictly related to the insulin receptor signaling, but also a specific aspect of lipid metabolism, which is the fatty acid  $\beta$ -oxidation, a catabolic process through which fatty acids are degraded to trigger citric acid cycle and produce energy, and whose impairment exacerbate insulin sensitivity by inducing a lipotoxic and inflammatory state, detrimental for intracellular insulin signal in skeletal muscle.

### **Cell line**

C2C12, a mouse skeletal muscle cell line, is an adherent diploid sub-clone of the mouse myoblast cell line established by David Yaffe [58]. C2C12 cell line was purchased from ATCC® (CRL-1772™) and cultured in base medium Dulbecco's Modified Eagle's Medium (DMEM) with 10% of FBS and  $1 \times 10^5$  U/L penicillin/streptomycin in a humidified condition in 5% CO<sub>2</sub> at 37°C. After 2 days of adhesion,  $3 \times 10^5$  C2C12 cells were seeded in 60 mm dishes and terminally differentiated to myocytes by switch to a differentiating medium (DMEM with 2% of HS,  $10 \times 10^5$  U/L penicillin/streptomycin, 1% insulin, transferrin, selenium [ITS]) for 48 hrs.

### **Cell synchronization**

C2C12 terminally differentiated to myocytes, were synchronized by switching to a DMEM supplemented with 50% horse serum, capable to induce a serum shock. After 2 hrs in serum-rich DMEM, cells were rinsed and re-fed with serum-free DMEM for 24 hrs. At the established time-points (every 4 hrs over a 24 hrs period) dishes were washed twice with ice-cold PBS 1X, lysed, and harvested in 1 mL TRIzol reagent (Life Technologies, Carsbald, California, United States) by scraping with a rubber policeman and RNA extracted from cell lysates. To verify cell synchronization, messenger oscillation of the molecular circadian clock components *Bmal1*, *Clock*, *Per1*, *Per2*, *Cry2* and protein oscillation of the molecular circadian clock component BMAL1, PER1, PER2, CRY2 were monitored during the 24 hrs period. The protein oscillation of CLOCK was not evaluated in the current study, since a previous *in vivo* study demonstrated that *Clock* knock out mouse models continue to exhibit a stable and autonomous peripheral circadian rhythm suggesting that CLOCK is not essential for the proper functioning of the transcriptional and translational feedback loop of the circadian clock [59,60]. **Figure 1A** schematically shows the serum shock protocol used for the cell synchronization.

### **RNA isolation and RT-qPCR**

Total RNA was extracted using TRIzol reagent (Life Technologies, Carsbald, California, United States). After cell centrifugation at 4°C to obtain the cell pellet, TRIzol was added to C2C12 pellet on ice and the pellet was carefully homogenized with pipet in eppendorf. After 15 min at room temperature (RT), 200 µl of chloroform were added and the eppendorf vortexed for 15 sec for 2 times with a pause of 2 min at RT. The mixture obtained was centrifuged at 12000xg for 15 min at 4°C and upper phase carefully transferred in a new clean eppendorf at RT. After measuring the volume obtained, a quantity of isopropanol equal to the half of the volume obtained and 1 µl of glycogen were added and the sample preserved overnight at -20°C. The day after, the sample was centrifuged at 12000xg for 10 min at 4°C and the supernatant eliminated with pipet. The pellet was washed with 1 ml 75% ethanol and centrifuged at 12000xg for 5 min at 4°C. This passage was repeated three times. Lastly, the pellet was dried for 10 min in sterile condition at RT and 20 µl RNase-free/sterile H<sub>2</sub>O were added keeping the samples at 4°C for 1 h. The dissolved pellet was then heated for 5 min at 65°C, its purity assessed by the A260/A230 absorbance ratio and the samples stored at -80°C until use. The cDNA synthesis was performed using the RT2 First Strand Kit, purchased from Qiagen® (Milan, Italy); this protocol requires a first treatment for 5 min at 42°C followed by 2 min on ice with buffer GE (5X genomic DNA elimination buffer) to eliminate potential genomic DNA contamination and, subsequently, a retro-transcription process for cDNA synthesis. In detail, starting from 1 µg RNA, the reverse transcription mix was prepared according

to the manufacture's instruction. The mix was incubated for 15 min at 42°C and subsequently, immediately stopped by incubation at 95°C for 5 min. To each reaction 180 µl RNase-free water were added and the sample of cDNA stored at -20°C until use. The cDNA was used for quantification of messenger levels of the clock genes under investigation for the study. The total reaction volume (12.5 µl) consisted of 5 µl of cDNA, 7 µl of TaqMan® Universal PCR Mastermix (Applied Biosystems, Branchburg, NJ, USA) and 0.5 µl of primers-probes (Applied Biosystems, Branchburg, NJ, USA). **Table 1S of supplementary material** shows primers and probes assay ID. RT-qPCR was performed with StepOne Plus Real-Time PCR System, using the standard protocol; briefly, after two initial heating steps at 50°C (2 min) and 95°C (10 min), samples were subjected to 40 cycles of denaturation at 95°C (15 sec) and annealing at 60°C (60 sec). All samples were assayed in duplicate. Values were normalized against the expression of the housekeeping gene 18S ribosomal RNA (18S). The relative expression of target genes was calculated using the comparative threshold method, denominated  $2^{-\Delta Ct}$ . To exclude contamination of the PCR mixtures, in parallel with cDNA samples, reactions were also performed in the absence of cDNA template.

## Drug

HC was purchased from Sigma Aldrich (Sigma Aldrich, Italy) and dissolved in 100% ethanol (EtOH). Stock solutions of HC at the concentration of  $10^{-3}$  M were stored at -80°C and freshly thawed prior the experiments. Serial dilutions were prepared in serum-free DMEM as recommended by manufacturer.

## Setting of time-points treatment

To establish the time-points of HC exposure, the beginning of the circadian cycle (Time 0 [T0]) was set with the beginning of serum shock and consistently with the “canonical model” [6], time-points treatment were established on the basis of clock genes circadian expression and in particular of *Bmal1* messenger expression. The *Bmal1* peak transcription level (acrophase), corresponding to the nadir of *Per* and *Cry* transcription levels, was considered to correspond to the early morning; conversely, the *Bmal1* nadir transcription level (bathyphase), corresponding to the *Per* and *Cry* peak transcription levels, was considered to correspond to the early evening in the daily rhythm. Time-point with medium *Bmal1* transcription level (midphase) was considered to resemble the afternoon in the daily rhythm [60,61].

## HC treatment schedule

HC concentrations administered to C2C12 cells corresponded to the mean serum cortisol concentrations observed in healthy human subjects [62] and AI patients treated with once-daily MR-HC and with thrice-daily of conventional IR-HC [47]. At the time-points of the cell circadian rhythm corresponding to 8 am, 1 pm and 6 pm of the subjective daily rhythm, C2C12 cells were exposed for 1 h (minimum time to observe GC genomic effects and maximum time to avoid drastic cells de-synchronization [19,63-65]) to different HC concentrations. HC concentrations used to mimic physiological circulating cortisol concentrations (standard cortisol profile) have been reported in the text as “treatment schedule A” (TSA), while concentrations used to mimic the circulating cortisol concentrations reached in AI patients treated with once-daily MR-HC were reported as “treatment schedule B” (TSB) (flat cortisol profile), and concentrations used to mimic the circulating cortisol concentrations reached in AI patients treated with thrice-daily of conventional IR-HC were reported as “treatment schedule C” (TSC) (steep cortisol profile) specifically at acrophase, midphase and bathyphase. **Figure 1B** shows a simplified representation of the *in vitro* HC exposure at different circadian time-points. **Table 1** shows the treatment schedules and the correspondence to the time-points of the circadian rhythm obtained after C2C12 synchronization.

### **RT-qPCR insulin resistance-related array**

RT2 Profiler PCR Array provided in 96-well plates, contained primer assays for 84 insulin resistance-related genes and 5 housekeeping genes (Mouse RT2 Profiler™ PCR Array Insulin Resistance kit, PAMM-156Z, Qiagen, Milan, Italy). In addition, 1 well contained a genomic DNA control, 3 wells contained reverse-transcription controls and 3 wells contained positive PCR controls. RT2 Profiler PCR Arrays were performed following the manufacturer’s recommendations. After centrifugation of RT2 SYBR® Green/ROX qPCR Mastermix (Qiagen, Milan, Italy), the PCR components were prepared in a 15 ml tube by adding 1250 µl 2X RT2 SYBR® Green qPCR Mastermix, 200 µl cDNA, 1050 µl H<sub>2</sub>O and dispensing 25 µl of this mix to each well of MicroAmp® Fast Optic 96-well (Applied Biosystem, Lincoln Centre Drive Foster City, United States) in order to charge 10 ng cDNA per well. The last six wells, containing positive controls, were charged with PCR components and RNase-free water. The plate was placed in StepOne Plus Real-Time PCR System, using a standard protocol; briefly, after two initial heating steps at 50°C (2 min) and 95°C (10 min), samples were subjected to 40 cycles of denaturation at 95°C (15 sec) and annealing at 60°C (60 sec). All samples were assayed in duplicate. Values were normalized against the arithmetic media of 5 housekeeping genes expression. Results are expressed as mean of three different experiments. Data analysis and validation were performed using the free online software

provided by the manufacturer's website (Qiagen, Milan, Italy). **Table 2S of Supplementary material** reports 84 insulin resistance-related genes both as gene symbol and gene name. The insulin resistance-related array could be categorized according to their specific function as follows: Insulin Signaling: *Akt3*, *Gys1*, *Igf1*, *Igf1r*, *Ikkkb* (*Ikkbeta*), *Insr*, *Irs1*, *Irs2*, *Map2k1* (*Mek1*), *Mapk3* (*Erk1*), *Mapk9* (*Jnk2*), *Mtor*, *Pde3b*, *Pik3ca* (*P110alpha*), *Pik3r1* (*P85alpha*), *Ppargc1a* (*Pgc-1alpha*), *Ptpn1* (*Ptp1b*), *Rps6kb1*, *Slc2a4* (*Glut4*), *Socs3*, *Srebf1*; Non-Insulin Dependent Diabetes Mellitus: *Adipoq* (*Acrp30*), *Hk2*, *Ikkkb* (*Ikkbeta*), *Insr*, *Irs1*, *Irs2*, *Mapk3* (*Erk1*), *Mapk9* (*Jnk2*), *Mtor*, *Pdx1* (*Ipf1*), *Pik3ca* (*P110alpha*), *Pik3r1* (*P85alpha*), *Slc2a4* (*Glut4*), *Socs3*, *Tnf*; Adipokine signaling: Adipokines: *Adipoq* (*Acrp30*), *Il6*, *Lep*, *Nampt*, *Retn*, *Serpine1* (*Pai-1*), *Tnf*; Receptors & Transporters: *Adipor1*, *Adipor2*, *Cd36*, *Lepr*, *Slc2a4* (*Glut4*), *Tnfrsf1a* (*Tnfr1*), *Tnfrsf1b*; Signaling downstream of adipokines: *Akt3*, *Chuk* (*Ikbka*), *Ikkkb* (*Ikkbeta*), *Irs1*, *Irs2*, *Jak2*, *Mapk9* (*Jnk2*), *Mtor*, *Nfkbia* (*Ikba*, *Mad3*), *Ppara*, *Ppargc1a* (*Pgc-1alpha*), *Rela*, *Socs3*, *Stat3*; Innate Immunity: *Casp1* (*Ice*), *Chuk* (*Ikbka*), *Ikkkb* (*Ikkbeta*), *Irs1*, *Irs2*, *Nlrp3*, *Nfkbia* (*Ikba*, *Mad3*), *Pycard* (*Tms1*, *Asc*), *Rela*, *Tlr4*; Inflammation: *Alox5*, *Casp1* (*Ice*), *Ccl12* (*Mcp-5*, *Scya12*), *Ccr4*, *Ccr5*, *Chuk* (*Ikbka*), *Cxcr4*, *Ifng*, *Ikkkb* (*Ikkbeta*), *Il1b*, *Il23r*, *Il6*, *Lta4h*, *Nlrp3*, *Olr1*, *Pycard* (*Tms1*, *Asc*), *Rela*, *Tnf*, *Tnfrsf1a* (*Tnfr1*), *Tnfrsf1b*; Apoptosis: *Pparg*, *Serpine1* (*Pai-1*), *Tnf*, *Casp1* (*Ice*), *Ikkkb* (*Ikkbeta*), *Irs2*, *Mapk9* (*Jnk2*), *Nfkbia* (*Ikba*, *Mad3*), *Nlrp3*, *Pycard* (*Tms1*, *Asc*), *Rela*, *Tnfrsf1a* (*Tnfr1*), *Jak2*, *Pik3ca* (*P110alpha*), *Socs3*, *Rps6kb1*, *Tnfrsf1b*; Metabolic pathways, including carbohydrate metabolism: *Cs*, *Gys1*, *Hk2*, *Pck1*, *Pdk2*, lipid metabolism: *Acaca*, *Acacb*, *Acs11*, *Acs14*, *Apoe*, *Cebpa*, *Cnbp*, *Fabp4*, *Fasn*, *Lepr*, *Lipe*, *Lpl*, *Ppara*, *Pparg*, *Ppargc1a* (*Pgc-1alpha*), *Scd1*, *Srebf1*, *Srebf2*, and metabolite transport: *Apoe*, *Cd36*, *Fabp4*, *Rbp4*, *Slc2a4* (*Glut4*), *Slc27a1*, *Ucp1*, *Vldlr*; Infiltrating Leukocyte Markers of macrophages: *Ccr5*, *Cxcr4*, *Adgre1*; Th1 cells: *Ccr5*, *Cd3e*, *Cxcr3*, *Il18r1*; Th2 Cells: *Ccr4*, *Cd3e*, *Crlf2* (*Tslpr*), *Il1r1*; Th17 Cells: *Ccr6*, *Cd3e*, *Il23r*. Genes expression levels were considered significantly modified (upregulated or downregulated) if absolute fold change of relative gene expression >2.0 and p-values <0.1 were detected.

### RT-qPCR genes variation validation

On the basis of RT-qPCR array gene expression changes, genes mainly involved in the skeletal muscle insulin receptor signaling, whose expression was determinant of insulin sensitivity, were chosen and validated through RT-qPCR in Sybr Green. The total reaction volume (25  $\mu$ l) consisted of 2  $\mu$ l of cDNA, 12.5  $\mu$ l of RT2 SYBR<sup>®</sup> Green/ROX qPCR Mastermix (Qiagen, Milan, Italy), 0.5  $\mu$ l of primers-probes (Applied Biosystems, Branchburg, NJ, USA) and 10  $\mu$ l of H<sub>2</sub>O. **Table 3S of Supplementary material** shows primers accession numbers. RT-qPCR was performed with

StepOne Plus Real-Time PCR System, using the standard protocol; briefly, after two initial heating steps at 50°C (2 min) and 95°C (10 min), samples were subjected to 40 cycles of denaturation at 95°C (15 sec) and annealing at 60°C (60 sec). All samples were assayed in duplicate. Gene expression levels were normalized against the expression of the housekeeping gene cyclophilin A. The relative expression of target genes was calculated using the comparative threshold method,  $2^{-\Delta Ct}$ . To exclude contamination of the PCR mixtures, in parallel with cDNA samples, reactions were also performed in the absence of cDNA template.

### **Protein isolation and Western Blot analysis**

C2C12 myocytes were seeded at a density of  $3 \times 10^6$  in 60 mm dishes and terminally differentiated for 48 hrs after 2 days of adhesion. After HC treatment, cells were lysed, and protein extracted as previously described [67]. Proteins from cell preparations were separated by 8% (according to protein's molecular weight to detect) SDS-PAGE and then electroblotted onto a nitrocellulose membrane for 1h in a TransBlot Bio-Rad apparatus. After a blocking treatment for 1h with 5% of milk, the nitrocellulose filters were probed overnight with primary antibodies specific for BMAL1 (#14020, Cell Signalling, Italy), PER1 (sc-398890, Santa Cruz Biotech, Inc), PER2 (GT5310, ThermoFisher, Italy), CRY2 (PA5-13125, ThermoFisher, Italy) to evaluate cell synchronization and confirm clock genes expression. Moreover, the molecular mechanisms investigated through western blot included not only the pathways strictly related to the insulin receptor signaling by analyzing intracellular levels of pIRS1 (Tyr608) (#09-432, Millipore, Italy), IRS1 (#2382, Cell Signalling, Italy), pAKT (Ser473) (#9271, Cell Signalling, Italy), AKT (#9272, Cell Signalling, Italy), but also the fatty acid  $\beta$ -oxidation catabolic process, which contributes to exacerbate skeletal muscle insulin sensitivity, by analyzing intracellular levels of pAMPK $\alpha$  (Thr172) (40H9) (#2535, Cell Signalling, Italy), AMPK $\alpha$  (#2793, Cell Signalling, Italy), pACC (Ser79) (D7D11) (#11818, Cell Signalling, Italy), ACC (C83B10) (#3676, Cell Signalling, Italy).  $\beta$ -actin (A4700; Sigma Aldrich, Italy) was used as endogenous control for protein expression analysis. Subsequently, filters were hybridized with peroxidase-conjugated secondary antibodies and immunoreactive bands were detected by ECL system. After chemiluminescent reaction, the blot was exposed to ImageQuant Las 4000 (GE Healthcare). Densitometry bands quantification was performed through ImageJ software.

### **Statistical analysis**

All the experiments were replicated at least three times. Statistical analyses of clock gene expression and C2C12 cells synchronization were performed using GraphPad Prism 5 software. Cosinor analysis was used to calculate the 24 hrs rhythmicity and to graphically reproduce the

presence of 24 hrs oscillations of clock genes across different time-points. In detail, Cosinor analysis was performed by fitting a periodic sinusoidal function  $f(t) = M + A \cos(\pi / 12 \cdot t - \Phi)$  to the expression value of each gene across the time-points, where  $f(t)$  is the gene expression levels in a given time-point,  $M$  Mesor is the midline estimating statistic of mean,  $A$  is the sinusoidal amplitude of oscillation,  $t$  is the time expressed in hrs and  $\Phi$  is the acrophase (peak time of the fitted cosine function). P values depicted in each graph were calculated by ANOVA. The expression of individual messenger by RT-qPCR array was analyzed using threshold cycle (Ct) values obtained with a threshold of 0.4. Ct values of 35 or greater for any messenger in either the control or the experimental samples was excluded from the analysis and marked as undetectable or undetermined. Data analysis was performed uploading the Ct values that passed through these stringent criteria on Qiagen web portal (<https://dataanalysis.qiagen.com/pcr/arrayanalysis.php>; Qiagen, Milan, Italy). Dose-time comparison of fold change were calculated by the software using the  $\Delta\Delta C_t$  method, calculating the fold change in terms of  $C_t$  values in each group of treatment, and relativized on five housekeeping genes expression levels. The Volcano plot analysis, combining the measure of statistical significance from the statistical test with the magnitude of the fold change, was used to evaluate the significant genes expression change. Gene expression levels were considered significant modified (upregulated or downregulated) whether absolute fold change of relative gene expression  $>2.0$  and p-values  $<0.5$  were detected. Features of interest are typically those in the upper left- and right-hand corners of the Volcano plot, as these have large fold changes (lie far from  $x=0$ ) and are statistically significant (have large y-values). Validation of downregulated genes, evaluated by RT-qPCR, was analyzed through ANOVA analysis followed by a multiple comparative test (Bonferroni, Newman-Keuls or Dunnett's correction).

## RESULTS

C2C12 cells, after a suitable synchronization, displayed a different response to the different doses of HC, depending on the time of exposure, particularly on the time-point of the cell circadian rhythm.

### **Rhythmic expression of clock genes in synchronized C2C12 cells**

The synchronization procedure clearly induced oscillation of the clock genes. Messenger expression of *Bmal1* peaked at 12 hrs and decreased, reaching the nadir, at 20 hrs time-points. Similarly, protein expression of BMAL1, that reached the highest levels at 12 hrs and the lowest levels around

20 hrs time-points. *Clock* messenger expression, although following a cyclic pattern, exhibited little periodicity. Conversely, messenger and protein expression of *Per1*, *Per2* and *Cry2* genes peaked at 24 hrs and decreased, reaching the nadir at 12 hrs. Based on these results and according to the commonly accepted circadian clock model, in order to set the *in vitro* exposure times, it has been assumed that the 12 hrs time-point correspond to the early morning (*Bmal1* acrophase), 15 hrs time-point roughly correspond to the afternoon (*Bmal1* midphase) while 20 hrs time-point represents the early evening of the daily rhythm (*Bmal1* bathyphase). **Figure 2A** shows the messenger expression profile of the clock genes during the 24 hrs period, whereas **Figure 2B** shows the protein expression profile of the clock genes during the 24 hrs whose densitometric measurement and the resulting graphs are shown in **Supplementary Figure 1**.

### **Expression analysis of 84 insulin resistance-related genes in synchronized C2C12.**

HC concentrations used to mimic circulating cortisol concentrations reached in AI patients treated with once-daily MR-HC (TSB) (flat cortisol profile) or treated with thrice-daily of conventional IR-HC (TSC) (steep cortisol profile) were compared each other and to HC concentrations used to mimic physiological circulating cortisol concentrations (TSA) (standard cortisol profile).

In the acrophase, TSB and TSC produced no relevant changes in the expression of various genes when compared to TSA or reciprocally. In detail, no significant change in gene expression has been detected when TSB was compared to TSA, although *Acs11*, *Ccr4*, *Chuk*, *Rbp4*, *Cd36* genes tended to be upregulated, without reaching a significant difference. Similarly, no significant change in gene expression has been detected when TSC was compared to TSA, although *Acs11*, *Ccr4*, *Chuk*, *Rbp4*, *Cd36*, *I118r1*, *I11b*, *Pdk2* genes tended to be upregulated, without reaching a significant difference, with the exception of one gene (*Chuk*), which was upregulated with a significant fold change of 2.65 ( $p=0.003$ ). No significant change in gene expression has been detected when TSB and TSC were compared reciprocally, although *Acs11* and *Chuk* genes tended to be downregulated and upregulated in TSB compared to TSC. **Figure 3A**, **3B** and **3C** show the volcano plot representations without significant gene expression changes after TSA, TSB and TSC in the acrophase.

In the midphase, TSB and TSC produced minor changes in the expression of various genes when compared to TSA or reciprocally. In detail, no significant change in gene expression has been detected when TSB was compared to TSA, although *Casp1*, *Ccl12*, *Lepr*, *Olr1* genes tended to be upregulated, without reaching a significant difference, with the exception of one gene (*Cs*), which was upregulated with a significant fold change of 3.17 ( $p=0.05$ ). Similarly, no significant changes in gene expression has been detected when TSC was compared to TSA, although *Cd36*, *Rbp4*, *Retn*

genes tended to be upregulated and *Pdk2* and *Pdx1* genes down-regulated, without reaching a significant difference, with the exception of one gene (*I118r1*), which was upregulated with a significant fold change of 3.18 ( $p=0.05$ ). Four genes (*Adipor2*, *Cs*, *Serpine1* and *Sic27a1*) were upregulated with a significant fold change of 2.08 ( $p=0.009$ ), 3.16 ( $p=0.0002$ ), 2.58 ( $p=0.01$ ) and 2.20 ( $p=0.005$ ), respectively, when TSB was compared to TSC. **Figure 4A, 4B** and **4C** show the volcano plot representations without significant gene expression changes, except for *Cs* and *I118r1*, after TSA, TSB and TSC in the midphase.

In the bathyphase, TSB and TSC produced a significantly different effect on expression of various genes when compared to TSA or reciprocally. Indeed, no significant change in gene expression has been detected when TSB was compared to TSA, whereas 38 different genes were downregulated and 1 gene was upregulated, when TSC was compared to TSA. **Figure 5A, 5B** and **5C** show the volcano plot representations of gene expression changes after TSA, TSB and TSC in the bathyphase. Particularly, **Figure 5B** and **Figure 5C** show the significant gene expression changes after TSB and TSC comparing to TSA in the bathyphase. Among the 39 regulated genes, the volcano plot analysis revealed the significant downregulation of 21 genes. **Table 2** details 21 genes significantly downregulated specifying fold changes and p-values. Similarly, 34 genes were downregulated when TSB was compared to TSC. Among the 34 regulated genes, the Volcano plot analysis revealed a significant downregulation of 22 genes, with a superimposable profile observed comparing TSC and TSA. **Table 3** details 22 genes significantly downregulated specifying fold changes and p-values. Moreover, **Figure 6** shows the heatmap of the all analyzed gene fold regulation in acrophase, midphase and bathyphase by representing each gene along the rows and the different treatment conditions along the columns. Among the genes significantly regulated during bathyphase when TSB and TSC were compared to TSA and reciprocally, as detailed above, *Insr*, *Irs1*, *Irs2*, *Pi3kca* and *Adipor2* gene expression were validated through Sybr Green RT-qPCR. No change in gene expression has been detected when TSB was compared to TSA, while when TSC was compared to TSA a strong and significant inhibition of *Insr* (\*\* $p<0.01$ ), *Pi3kca* (\*\*\*\* $p<0.0001$ ) and *Adipor2* (\*\* $p<0.01$ ) expression and a marked, but not significant, inhibition of *Irs1* and *Irs2* occurred. **Figure 7** shows the expression levels of *Insr*, *Irs1*, *Irs2*, *Pi3kca*, *Adipor2* after TSA, TSB and TSC in bathyphase.

### **Analysis of intracellular insulin receptor signaling and fatty acid $\beta$ oxidation pathway**

Considering the huge and different effect observed on gene expression and induced during the bathyphase by TSB and TSC compared to TSA, the analysis of intracellular proteins involved in insulin sensitivity, particularly in insulin receptor signaling and in fatty acid  $\beta$  oxidation pathway

has been performed only in C2C12 during the bathyphase. TSB and TSA induced similar intracellular protein modifications. Conversely, TSC strongly affects intracellular insulin receptor signaling and fatty acid  $\beta$ -oxidation pathway. **Figure 8** shows that TSC inhibited IRS1 phosphorylation at Tyr608 and AKT phosphorylation at Ser473, as well as AMPK $\alpha$  phosphorylation at Thr172 and ACC phosphorylation at Ser79. **Figure 9** shows a graphic representation of the investigated intracellular insulin receptor signaling and fatty acid  $\beta$ -oxidation pathway in the skeletal muscle.

## DISCUSSION

The current study explores the effect of the exposure of HC, administered at concentrations inducing either non-physiological or physiological daily cortisol profiles, at different phases of the circadian rhythm, on insulin sensitivity, in an *in vitro* model of mouse skeletal muscle cell. In particular, the treatment with non-physiological HC concentration (TSC, inducing a circulating daily cortisol profile resembling that reached in AI patients treated with thrice-daily of conventional IR-HC with a steep cortisol profile), during bathyphase, the time-point of cell circadian rhythm corresponding to the early evening, is associated with an impairment of insulin sensitivity, which is not occurring during treatment with physiological HC concentrations TSB and TSA, which induce a circulating daily cortisol profile resembling that reached in AI patients treated with once-daily MR-HC or in healthy subjects, respectively. At molecular level, during bathyphase, compared to either TSB or TSA, TSC induced downregulation of the expression of several genes involved in the regulation of insulin sensitivity and, particularly, in the regulation of intracellular insulin receptor signaling and fatty acid metabolism, particularly fatty acid  $\beta$ -oxidation, whose impairment contributes to the development of insulin resistance. Conversely, non-physiological and physiological HC concentrations, during acrophase and midphase, the time-points of cell circadian rhythm corresponding to the early morning and the early afternoon, did not significantly affect insulin sensitivity, suggesting that GCs exposure affects insulin sensitivity and consequently insulin-dependent glucose, lipid and protein metabolisms in a manner which is strictly associated with the cell circadian rhythm in skeletal muscle.

Advances in the scientific knowledge of the cellular and molecular underpinnings of the cell circadian rhythm indicate that a main biological clock controls a wide range of physiological processes by acting through the circadian clock machinery, located in SCN (master clock) and in

several peripheral locations (peripheral clocks) [1,2]. In humans, SCN cells cyclically stimulate paraventricular nucleus (PVN) neurons, through direct and indirect axonal projections, leading to a circadian release of cortisol-releasing hormone and, consequently, adrenocorticotrophic hormone (ACTH) and cortisol, the main endogenous GC, which, in turn, contributes to trigger oscillation of peripheral clocks. Indeed, the circadian clock regulates cortisol secretion, rhythm and action, acting at different levels of the HPA axis, including at the level of GC receptors, whereas GCs are able to modulate the activity of the circadian clock, through the regulation of the expression and oscillation rhythm of clock genes and proteins, in a reciprocal interplay [60,61].

The interplay between HPA axis and circadian clock has been demonstrated by evidence derived from *in vitro* and *in vivo* studies in animal and/or human models [9–21].

Several rodent cell circadian clock knockout and mutant models demonstrated the role of cell circadian clock on the regulation of corticosterone circadian release and rhythm, through the modulation of HPA axis, in *in vivo* studies. *Bmal1* knockout mouse models displayed loss of ACTH and corticosterone circadian release, with ACTH drawing a flat daily curve and corticosterone drawing a peaked curve, with higher nocturnal peak [9]. *Per1* and *Per2* knockout mouse models displayed loss of corticosterone circadian release, drawing a flat daily curve with corticosterone constantly persisting at high levels during the entire day [10]. *Cry1* and *Cry2* knockout mouse models displayed low levels of corticosterone associated with a different peaked daily curve; while *Cry2* knockout mice showed a more physiological trend, with a peak in the first hours of the night, *Cry1* knockout mice showed a premature peak of about 2 hrs [11], suggesting a *Cry1*-dependent more than *Cry2*-dependent control of corticosterone circadian rhythm. *Clock* mutant mice displayed loss of corticosterone circadian release, drawing a flat daily curve with corticosterone constantly persisting at low levels during the entire day [12], while *Per2/Cry1* double mutant mice displayed loss of ACTH and corticosterone circadian release, drawing a flat daily curve, together with a blunting of corticosterone to ACTH challenge [13]. Moreover, in CD patients the circadian expression of the clock genes *CLOCK*, *BMAL1*, *CRY1*, *PER1*, *PER2*, *PER3* was abolished, unlike what was found in the group of healthy control subjects, in which all the clock genes analyzed showed a physiological circadian trend [14].

Moreover, the cell circadian clock has been demonstrated to regulate not only GC secretion and rhythm, but also GC action, through the modulation of GC receptor, both in animal and human *in vitro* studies. In particular, the main components of circadian clock, such as *CRY1/2* and *CLOCK/BMAL1* have been demonstrated to blunt or repress GC receptor activity [15-17]. Indeed, in mouse embryonic fibroblasts primary cultures, *CRY1/2* competed with GCs for the binding to

GC receptor with blunting of the receptor activation and alteration of transcriptional response to GCs. Particularly, CRY interacts with the carboxy-terminus of GCs receptor, which is required for either activation or repression of transcription in response to ligand [15]. In human cancer cell lines, CLOCK/BMAL1 repressed GC receptor activity by acetylating multiple lysine residues of GC responsive element (GRE)-binding sequence, with consequent blunting of the binding of GC receptor to GRE of the receptive genes [16]. In human peripheral blood mononuclear cells, CLOCK triggers the acetylation of multiple lysine residues located in GC receptor hinge region, an important region involved in hormone binding, receptor activation and/or intracellular signaling, at the highest level in the early morning and at the lowest level in the late evening, with the determination of the physiological circadian GCs sensitivity variation, with a lower sensitivity in the morning and a higher sensitivity in the night [17].

On the other hand, the role of HPA axis on the regulation of cell circadian clock, and consequently, circadian rhythm, has testified by studies evaluating the effect of exogenous GCs in the regulation of expression of circadian clock machinery, in both animal and human *in vitro* and/or *in vivo* studies. Indeed, in rat non-synchronized fibroblast cell line, 1h exposure to 100 nM dexamethasone, a synthetic exogenous long-acting GC, induced a cell circadian rhythm, particularly of *Per1/3* and *Cry1*, with the classical 22 hrs period, which was spontaneously maintained for the two cycles [18], suggesting that GCs can efficiently induce an *in vitro* cell synchronization. In human adipocytes primary cultures with an autonomous, spontaneous, physiological *in vitro* cell circadian rhythm, 2 hrs exposure to 1000 nM dexamethasone reduced the period of circadian rhythm of clock, especially of *CLOCK*, *BMAL1*, and *PER2*, from 24 hrs to 22 hrs, when exposed at the time corresponding to the early morning [19], suggesting that GCs can modify a pre-existing *in vitro* cell synchronization. Moreover, in mice subjected to surgical ablation of SCN, the administration of  $7 \times 10^5$  nM dexamethasone, in the early morning, modulated the expression of almost 60% of the circadian genes in the liver; in particular, dexamethasone induced or repressed circadian clock gene expression, particularly of *Bmal1*, *Per1* and *Cry1* and the immediately downstream gene clusters involved in clock-controlled liver functions, in a non-rhythmic background, re-synchronizing the cell circadian rhythm [20]. Similarly, in adrenalectomized rats, the physiological corticosterone replacement, performed in order to induce the physiological circadian corticosterone rhythm, with high circulating levels during the night and low circulating levels during the day, may restore in the amygdala the cell circadian rhythm, particularly of *Per2*, previously abolished by the removal of adrenal glands [21]. These two latter studies on animal models, lacking the physiological cell circadian rhythm and an intact HPA axis, clearly demonstrated that GCs might induce or modulate the cell circadian rhythm expression and function and induce cell synchronization even in the

absence of the main central or peripheral organs deputed to the generation and regulation of physiological clock system. Altogether, these *in vitro* and *in vivo* animal and/or human models suggest the presence of an intricate interplay existing between the circadian clock and HPA axis, especially GCs circadian production, rhythm and actions; notably, these actions are multiple and include the regulation of glucose, lipid and protein metabolisms together with insulin sensitivity, whose impairment, consequent of disruption of cell circadian clock or HPA axis, determines the development of insulin resistance and consequent metabolic disorders.

Insulin resistance is a clinical condition characterized by the inability of insulin to regulate the circulating levels of plasma glucose through the suppression of hepatic glucose production and the stimulation of peripheral glucose utilization, especially in skeletal muscle; it is generally the consequence of a defect of insulin receptor signaling caused by downregulation of the expression, as well as gene mutations or post-transcriptional and/or post-translational modifications of insulin receptor and/or downstream effector molecules, mainly IRS-1 and IRS-2, which, in the skeletal muscle, are phosphorylated on the tyrosine or serine residues, therefore influencing positively or negatively, respectively, the intracellular transmission of the insulin signal [36]. Persistent peripheral insulin resistance initially induces a compensative increase of insulin secretion by pancreatic  $\beta$ -cells, but lastly induces a gradual dysfunction and death of the pancreatic  $\beta$ -cells, triggering to the development of diabetes. In addition to the impairment of glucose metabolism, an impairment of lipid metabolism also occurs, with the increase of circulating free fatty acids levels, induced by their excessive release from adipose tissue, and captured by skeletal muscle, where they accumulate into the cytoplasm of the cells, for the concomitant impairment of their mitochondrial  $\beta$ -oxidation, inducing a lipotoxic state due to lipid infiltration. The lipotoxic state is responsible for the exacerbation of the impairment of insulin receptor activity, directly and indirectly, through the induction of an inflammatory state, and it is secondary responsible for a decrease of amino acid incorporation protein synthesis, determining a catabolic state with predominance of protein degradation in skeletal muscle [36].

Several *in vitro* and *in vivo* studies in animal and/or human models have demonstrated that GCs directly regulate glucose, lipid and protein metabolisms, by different mechanisms, including the well-known interference with the insulin receptor signaling, with consequent impairment of insulin sensitivity and development of insulin resistance, which contributes not only to the development of an impairment of glucose tolerance, but also to the shift from muscle protein synthesis to muscle protein degradation and from anabolic to catabolic state [22-27,37]. These mechanisms are emphasized in condition of GC excess, including exogenous and endogenous CS, where skeletal muscle protein catabolism together with insulin resistance determines a progressive muscle atrophy

and a systemic metabolic disorder [22-27,37]. Indeed, in mouse skeletal muscle cell line and in primary cultures of human myoblasts, 24 hrs exposure to 1000 nM dexamethasone antagonized insulin action through a decrease of IRS-1 expression and an increase of IRS-1 phosphorylation on serine residues, inducing an impairment of insulin receptor signaling and, consequently, insulin sensitivity [22]. In primary cultures of human myocytes, 48 hrs GCs exposure significantly reduced intracellular insulin receptor signaling and, consequently, glucose uptake [23]. On the other hand, in mice displaying a reduction of corticosterone production, induced by a selective inhibitor of 11  $\beta$ -hydroxysteroid dehydrogenase type 1 (11  $\beta$ -HSD1), the key enzyme that converts the inactive 11-dehydrocorticosterone to the active corticosterone, the insulin action is agonized through an increase of IRS-1 phosphorylation on tyrosine residues, inducing an improvement of insulin receptor signaling and, consequently, insulin sensitivity in skeletal muscle, with a consequent decrease in circulating fasting glucose levels [22]. Moreover, in adrenalectomized diabetic mice, the exposure to 20  $\mu$ g *pro* kg of body weight/day dexamethasone induced a concomitant skeletal muscle impairment of insulin receptor signaling and degradation of protein; in particular, dexamethasone induces a competition of active GC receptor with IRS-1 for the association with phosphatidylinositol 3 kinase (PI3K), with consequent impairment of insulin signaling, due to IRS-1 displacement from PI3K, and the activation by the complex GC receptor/ PI3K complex of protein degradation [24]. In healthy human subjects, the administration of 2 mg dexamethasone in four daily doses for 2 days induced an impairment of insulin receptor signaling and insulin action by affecting lipid metabolism, with decrease of fatty acid  $\beta$ -oxidation and increase of lipolysis, with consequent lipid accumulation and decrease of glucose uptake in skeletal muscle, and systemic hyperglycemia [25]. Moreover, a similar study on healthy human subjects demonstrated that the administration of 500 mg dexamethasone, in four daily doses for 2 days, induced skeletal muscle insulin resistance associated with compensatory hyperinsulinemia [26]. Importantly, the overnight HC infusion at a concentration inducing a short term hypercortisolemia in healthy human subjects preserving  $\beta$ -cells function, induced a systemic insulin resistance characterized by hyperglycemia and high levels of circulating free fatty acids accompanied with higher insulinemia [27]. Currently, little is known about the molecular mechanisms underlying the effect of GCs excess, and particularly, the loss of the physiological cortisol circadian rhythm on the development of metabolic disorders, also due to the inexistence of specific models, although a role of the disruption of cell circadian clock and rhythm has been suggested.

Some evidences in *in vivo* animal and human models suggest the disruption of cell circadian clock to mediate the GCs effects on glucose metabolism and insulin sensitivity, through the regulation of cell circadian clock machinery component expression. Indeed, mice with deletion of genomic GRE

in the *Per2* gene were protected from the dexamethasone-induced development of skeletal muscle and adipose insulin resistance and impairment of glucose tolerance [28]. Interestingly, several *in vivo* evidences in animal and human models recently demonstrated a strict link between cell circadian clock disruption and insulin resistance and consequent glucose intolerance or diabetes [29-34]. Indeed, *Bmal1* knockout mice developed glucose intolerance or diabetes, with the increase in fasting glucose levels accompanied by a reduction in insulin secretion, due to an impairment in insulin secretion pathway in  $\beta$ -cells of the pancreas [29]. *Clock* mutant mice developed not only hyperphagia, associated with upregulation of two potent orexigenic peptides, orexin and ghrelin, and consequent obesity associated with hyperleptinemia, but also hyperglycemia and hyperlipidemia [30]. *Per2* knockout mice developed hyperphagia, likely consequent to the loss of circadian feeding rhythm leading to equal food intake during both the light and dark daytime, and consequent obesity [31]. On the other hand, in humans, a *CRY2* allele variant, due to a single nucleotide polymorphism, has been associated with impairment of glucose tolerance or diabetes in the general population of European and Asiatic cohorts of subjects [32]. Moreover, a circadian rhythm misalignment, obtained by forcing behavioral habits of healthy male subjects with an abrupt shifting of their normal circadian rhythm by 12 hrs, impairs skeletal muscle insulin sensitivity, with consequent increase of fasting glucose, due to decreased insulin-stimulated glucose disposal and uptake [33]. These studies demonstrated the important role of circadian clock in the control of glucose metabolism. Interestingly, a study on adipose tissues derived from a population of obese women demonstrated that adipocyte non-physiological fluctuation components belonging to the circadian clock, represented by increased circadian variability of *BMAL1* and *PER2* expression, was associated with an increased sagittal diameter of the respective women abdomen, marker of visceral obesity, demonstrating that the impairment of the circadian clock might be associated with metabolic syndrome [34]. Furthermore, recent studies demonstrated that a huge number of skeletal muscle genes follows a circadian expression influencing a wide range of physiological functions including not only muscle-specific functions, such as myogenesis, fiber-type shifts, and mitochondrial respiration, but also metabolic functions, such as glucose tolerance and insulin sensitivity [68,69], therefore confirming that skeletal muscle, the key metabolic tissue responsible for the great majority of insulin-mediated whole-body glucose uptake and disposal, is subject to circadian control, and regulates glucose metabolism and insulin sensitivity in a circadian manner.

The totality of these studies suggests that a GC excess might be directly and indirectly responsible for the development of insulin resistance, due to a relevant impairment of insulin receptor signaling and insulin receptor mediated intracellular glucose, lipid and protein metabolisms, mainly in the skeletal muscle; these evidences are also confirmed in the pathological human *in vivo* model of CS.

Indeed, CS is associated with insulin resistance, and consequent development of glucose intolerance and/or diabetes [37]. The mechanisms underlying these events include the impairment of the insulin receptor signaling, operated by GCs directly, or indirectly through the stimulation of lipolysis and proteolysis and the consequent increase of fatty acids and amino acids, inducing the development of metabolic syndrome, characterized not only by glucose intolerance, but also by dyslipidemia and catabolic state [37]. The GCs effect on adipose tissue, with the consequential development of visceral obesity, which emphasizes the metabolic syndrome, as well as the concomitant GCs effect on pancreatic  $\beta$ -cell, with the inhibition of insulin secretion, are probably responsible for the development of diabetes in CS [37].

Conversely, AI, characterized by cortisol deficiency and by a complete loss of cortisol circadian rhythm, requires lifelong GC replacement therapy [38]. Before the availability of synthetic GCs, the great majority of AI patients died within a year or at most two from the diagnosis, mainly due to adrenal crisis [39]. The introduction of GC replacement therapy, in the early 1950s, changed the AI management, reducing morbidity and mortality [41-45]. However, AI patients maintained a mortality rate higher than that associated with the general population [41,42], together with a higher morbidity for metabolic disorders, as well as cardiovascular, infectious, immune and skeletal diseases, resulting in an impaired quality of life [38-39]. This considerable morbidity and mortality may be partially attributable to the disruption of GC circadian rhythmicity induced by the conventional GC formulations [43-46]. Indeed, the most commonly used conventional IR-HC thrice daily treatment schedule is associated with a non-physiological cortisol daily pattern, not providing an adequate GCs physiological replacement therapy, mainly due to the high circulating cortisol levels in the evening [47-55]. Recently, the novel MR-HC formulation appeared able to improve metabolic, as well as cardiovascular, immune and skeletal complications, with positive impact on quality of life when compared with conventional GC formulations [47-55].

However, the specific role of non-physiological daily cortisol profile or circadian cortisol rhythm on the development of insulin resistance and the underlying molecular mechanisms, in the skeletal muscle, remains a major challenge.

The current study, for the first time, elucidated the metabolic effects of HC exposure, at different concentrations, in different time-points of the cell circadian rhythm by exploring the molecular mechanisms both at genomic and protein levels, in a synchronized *in vitro* model. In the current study, in order to determine the role of cell circadian rhythm in the HC-induced metabolic function, cell synchronization of the skeletal muscle cells C2C12 has been assessed by serum-shock protocol; this protocol efficiently induced the circadian expression of the main components of the clock

machinery and allowed to fix the time-points of treatment with HC. Previous reports have found that the addition of serum-rich media to cultured mammalian cells triggers the rhythmic expression of cell circadian clock, given the largely demonstrated presence of cell autonomous circadian clock, regardless of their species of origin [70]. In particular, as previously demonstrated in different *in vitro* models [70,71], despite the murine origin, in C2C12 cells, serum shock induced circadian clock rhythmic expression, by resetting endogenous clock genes expression, and its reactivation in a circadian manner [70]. The rhythmic oscillation of clock genes through the 24 hrs period allowed to establish the circadian time-points of treatment, which, for the purpose of the study, have been set at *Bmal1* acrophase, midphase and bathyphase, corresponding to maximum, medium and minimum expression levels, respectively. The circadian clock consists of an autoregulatory transcriptional/translational feedback loop mechanism with a positive and a negative arm; this mechanism predicts that the expression levels of *Bmal1*, the main effector of the loop mechanism positive arm, are at the highest levels in the first hours of light and at the lowest levels in the first hours of dark, with an opposed trend for *Per* and *Cry* expression levels, the main effectors of the loop mechanism negative arm, whose levels are highest in the first hours of dark and lowest in the first hours of light [7,8]. Starting from these observations, 12 hrs after serum shock high *Bmal1* and low *Per* and *Cry* expression was observed, while 20 hrs after serum shock a reversal trend was observed, as previously demonstrated in the same cell model [70]. Assuming 12 hrs after serum shock as corresponding to the early morning, 15 hrs after serum shock corresponding to the early afternoon and 20 hrs after serum shock corresponding to the early evening, different treatment schedules of HC exposure, inducing different physiological or pathological circulating cortisol daily curves: in particular, TSB and TSC, corresponding to HC concentrations used to mimic circulating cortisol concentrations reached in AI patients treated with once-daily MR-HC and thrice-daily of conventional IR-HC, respectively, were compared to TSA, corresponding to HC concentrations used to mimic physiological circulating cortisol concentrations in healthy subjects, specifically at the different cell circadian rhythm time-points acrophase, midphase and bathyphase. After the different treatment schedules, gene expression levels of 84 genes involved in the modulation of insulin sensitivity, and the development of insulin resistance, were evaluated and compared through genomic array, to obtain a first evaluation of HC exposure genomic effects on skeletal muscle insulin sensitivity in the three different cell circadian time-points. In detail, TSB and TSC, when compared to TSA during acrophase and midphase, did not significantly influence expression levels of genes involved in the regulation of insulin sensitivity, despite the relatively high HC concentrations. Conversely, TSC, but not TSB, during bathyphase, induced a significant downregulation in the expression of 21 main genes involved in the regulation of insulin sensitivity,

despite the relatively low concentrations of HC. An in-depth study of the function of these 21 genes showed their involvement in the regulation of intracellular insulin receptor signaling and a specific intracellular pathway of lipid metabolism, namely fatty acid  $\beta$ -oxidation. These interesting novel results demonstrated that the exposure of skeletal muscle cells to a low concentration of HC during the cell bathypahse, which typically occurs in the early evening of the physiological circadian rhythm, can strongly and negatively influence the intracellular transmission of insulin signal, disrupting the expression of the main genes involved in the regulation of insulin sensitivity, pointing out that the day-time, more than the degree, of HC exposure negatively influence insulin sensitivity in the skeletal muscle. Indeed, although the HC concentration used in TSC was only slightly higher than the HC concentrations used in TSB and TSA during bathyphase, a great number of genes involved in the regulation of insulin sensitivity was negatively regulated, whereas in acrophase and midphase, although the HC concentrations used in TSB and TSC were notably higher than the those used in TSA, no significant changes have been observed among the three different HC administration schedules, in the expression of genes involved in the regulation of insulin sensitivity, therefore emphasizing that the metabolic GCs effects depend on the different phases of cell circadian rhythm, probably as a consequence of the effect of the circadian clock on the GC action, mediated by the change in GC receptor sensitivity.

This evidence is confirmed by the data available in the literature on the different effect of various HC formulations inducing non-physiological or physiological cortisol profile, resembling or not the physiological cortisol rhythm. Indeed, AI patients treated with thrice daily conventional formulations, especially IR-HC, and exposed to the non-physiological cortisol pattern, when switched to once daily MR-HC therapy, able to better mimic the circadian cortisol profile, showed improvements in metabolic parameters, including body weight, waist circumference, lipid profile and, particularly, glucose metabolism, with reduction in fasting glucose and glycated hemoglobin in diabetic patients, reduction in insulin levels and insulin resistance in pre-diabetic patients, and a reduction in fasting glucose, glycated hemoglobin, insulin levels and insulin resistance in non-diabetic patients [47-55]

Moreover, in the current study, to better investigate the involvement of the 21 genes significantly downregulated in skeletal muscle insulin resistance during bathyphase, the five genes mainly involved in the regulation of insulin sensitivity (*Insr*, *Irs1*, *Irs2*, *Pi3kca* and *Adipor2*) were selected and re-analyzed through RT-qPCR, confirming their decreased expression exclusively after TSC exposure, and that, rather than the HC doses, the specific time-point of the circadian rhythm, at which they are administered, is the major responsible of the disruption in the transmission of the insulin signal. The confirmation of the downregulation of these genes allowed to perform an

additional molecular analysis, at protein level, to better investigate the intracellular insulin signal activation after the treatment schedules at cell bathyphase, the only time-point of the cell circadian rhythm with significantly relevant change in gene expression. In detail, the analysis of intracellular proteins involved in the insulin receptor signaling and in the fatty acid  $\beta$ -oxidation pathway corroborated the results obtained at genomic level. Indeed, following the pathological TSC schedule, insulin signaling was weakened as demonstrated by the strong inhibition of phosphorylated IRS1 at Thr608 (insulin receptor activating phosphorylation) and of phosphorylated AKT at Ser473 (intracellular insulin pathway activation), compared to insulin signaling activated by physiological TSA and TSB. Moreover, the concomitant inhibition of AMPK $\alpha$  phosphorylation at Thr172 and of ACC at Ser79 in TSC compared to TSB and TSA suggested that HC supra-physiological TSC during bathyphase might inhibit fatty acid  $\beta$ -oxidation, compared to physiological TSA and TSB.

The current study presents some limitations concerning the *in vitro* study of cell circadian rhythm. Although the oscillation of the clock genes is maintained at the peripheral level, in this *in vitro* system, the SCN input as well as the pharmacokinetics parameters regulating HC exposure *in vivo*, are missed. *In vivo* cortisol circulating levels and bioavailability are strongly affected by protein binding activity, metabolism and excretion in urine among the individuals, making it impossible to predict in an *in vitro* system. However, although the concentrations of cortisol may vary between individuals the pattern of cortisol circadian rhythm is sufficiently reproducible [72]. Moreover, the *in vitro* exposure to HC for only one hour in order to avoid the cell desynchronization and the loss of the *Bmal1* acrophase, certainly did not allow to investigate the gene and protein modifications that would have occurred with a more prolonged treatment. Despite these limitations, these current findings might support the clinical knowledge about cortisol circadian rhythm disruption and metabolic comorbidities.

## CONCLUSIONS

In conclusion, the current study demonstrated that TSC, inducing a circulating cortisol profile resembling that reached in AI patients treated with thrice-daily conventional IR-HC with a steep cortisol profile, during bathyphase, corresponding to the early evening in the daily rhythm, significantly induces insulin resistance by downregulating expression of genes particularly involved in insulin sensitivity in skeletal muscle. In particular, the significant downregulation of the main genes involved in the regulation of insulin sensitivity as well as the impaired intracellular insulin

receptor signaling accompanied to the inhibition of lipid oxidation pathway demonstrated that exposure to non-physiological concentrations of HC in the early evening may strongly affect insulin sensitivity. The current study, despite the limitations of an *in vitro* study, could support the current scientific literature highlighting the correlation between cortisol circadian rhythm disruption and metabolic disorders, as well as the metabolic improvements obtained using the new MR-HC formulation, which better mimic the circadian cortisol profile by reducing diurnal cortisol peaks and troughs and in particular by reducing the early evening cortisol overexposure.

Accepted manuscript

## LEGENDS TO THE TABLES AND FIGURES

### **Table 1. Treatment schedule after C2C12 synchronization.**

Synchronized C2C12 cells have been treated with different concentrations of HC to mimic circulating cortisol concentrations observed in healthy human subjects [63] and the serum cortisol peaks (expressed in nmol/L) in AI patients treated with once-daily MR-HC or thrice-daily IR-HC conventional treatments [48]. 12 hrs post serum free medium replacement, corresponding to *Bmal1* acrophase, resembled the 8 am in the daily rhythm; 15 hrs post serum free medium replacement, corresponding to *Bmal1* midphase, resembled the 1 pm in the daily rhythm; 18 hrs post serum free medium replacement, corresponding to *Bmal1* bathyphase, resembled the 6 pm in the daily rhythm. TSA: treatment schedule A; TSB: treatment schedule B; TSC: treatment schedule C.

### **Figure 1**

**Simplified representation of the *in vitro* synchronization protocol and of TSA and TSC performed in the different circadian time-points.** A) C2C12 myoblasts were seeded in 60 mm dishes and terminally differentiated to myocytes. After 48 hrs, the medium was changed and C2C12 were synchronized using DMEM-supplemented with 50% horse serum (serum shock). After 2 hrs in serum-rich, cells were rinsed and re-fed with serum-free DMEM for 24 hrs. B) At the indicated times (every 4 hrs over a 24 hrs period) dishes were washed twice with ice-cold PBS 1X, lysed, and RNA extracted from cell lysates. At each time-point of the cell circadian cycle, corresponding to 8 am, 1 pm and 6 pm of the subjective daily rhythm, C2C12 cells were exposed to different HC concentrations for 1h.

### **Figure 2**

**Circadian messenger and protein expression profile of *Bmal1*, *Clock*, *Per1*, *Per2* and *Cry2* in C2C12 cell line.** A) Double plotted graphs illustrating the temporal rhythm organization of *Bmal1*, *Clock*, *Per1*, *Per2* and *Cry2* in synchronized C2C12 cell line during 24 hrs. The messenger expression levels were normalized against the housekeeping gene *RNA18S*. Values represent the mean  $\pm$  SEM of six independent experiments. P values depicted in each graph were calculated by ANOVA. B) Protein expression profile of clock genes during 24 hrs. Proteins were normalized against b-actin. The blot is representative of two or three independent experiments. Densitometry protein bands quantification was reported in Supplementary data (Figure 1S).

### **Figure 3**

**Volcano plot representation indicates the statistical significance of gene expression changes comparing the exposure to several HC concentrations at acrophase time point of circadian rhythm.** A) Comparison between TSA vs TSB. B) Comparison between TSA vs TSC. C) Comparison between TSB vs TSC. The x-axis of the Volcano plot shows the log<sub>2</sub> of the fold-

differences, while the y-axis their p-values based on student's t-test. Symbols in the volcano plot above the dashed line readily identify fold-differences. The plot represents the mean of three independent experiments.

#### Figure 4

**Volcano plot representation indicates the statistical significance of gene expression changes comparing the exposure to several HC concentrations at midphase time point of circadian rhythm.** A) Comparison between TSA vs TSB. B) Comparison between TSA vs TSC. C) Comparison between TSB vs TSC. The x-axis of the Volcano plot shows the log<sub>2</sub> of the fold-differences, while the y-axis their p-values based on student's t-test. Symbols in the volcano plot above the dashed line readily identify fold-differences. The plot represents the mean of three independent experiments.

#### Figure 5

**Volcano plot representation indicates the statistical significance of gene expression changes comparing the exposure to several HC concentrations at bathyphase time point of circadian rhythm.** A) Comparison between TSA vs TSB. B) Comparison between TSA vs TSC. C) Comparison between TSB vs TSC. The x-axis of the Volcano plot shows the log<sub>2</sub> of the fold-differences, while the y-axis their p-values based on student's t-test. Features of interest are typically those in the upper left and right hands corners of the volcano plot, as these have large fold changes (lie far from x=0) and are statistically significant (have large y-values). ([www.qiagenbioinformatics.com](http://www.qiagenbioinformatics.com)). Plots circled in red indicate significantly modified genes. The plot represents the mean of three independent experiments.

#### Figure 6

**Representation of 84 insulin resistance-related genes expression profile after several HC concentrations exposure at acrophase, midphase and bathyphase time points of circadian rhythm. Heatmap:** each gene is represented by a row while the columns show the fold regulation of genes expression (high fold regulation in green and low fold regulation in red) after the different treatments at the 3 time-points. A) TSA vs TSB at acrophase; B) TSA vs TSC at acrophase; C) TSA vs TSB at midphase; D) TSA vs TSC at midphase; E) TSA vs TSB at bathyphase; F) TSA vs TSC at bathyphase. The heatmap represents the mean of three independent experiments.

#### Table 2

**Gene symbols and name of 21 genes significantly downregulated during bathyphase when TSA was compared to TSC.**

### Table 3

**Gene symbols and name of 22 genes significantly downregulated during bathyphase when TSB was compared to TSC.**

### Figure 7

**Insulin pathway genes validation through RT-qPCR.** Values represent the mean  $\pm$  SEM of three independent experiments. The expression levels are normalized against the housekeeping gene cyclophilin. \*\* $p < 0.01$ ; \*\*\* $p < 0.001$  vs control.

### Figure 8

**Intracellular insulin signaling after different HC concentrations at bathyphase time point.** The blots are representative of three independent experiments. The values of densitometry reported are the mean  $\pm$  SEM of three independent experiments.

### Figure 9

**Schematic representation of intracellular insulin signaling and fatty acid  $\beta$  oxidation pathway activated by TSC in bathyphase of *Bmal1*** (Created with BioRender.com). Exposure of muscle cells to TSC HC in bathyphase strongly inhibits pIRS-1 Tyr608, thus decreasing intracellular insulin signaling. Concurrently, TSC in the same-time point, inhibits pAMPK Thr172, triggering to phosphorylation of ACC on Ser79 that increases its enzymatic activity, thus leading to an upregulated fatty acid synthesis.

### Statements:

**Statement of ethics:** According to the Ethical Committee of Federico II University, for the current experimental study on cell line no ethical approval was required.

**Conflicts of interest:** R.P. has been Principal Investigator of Research Studies for Novartis, HRA Pharma, Ipsen, Shire, Corcept Therapeutics, Cortendo AB; Co-investigator of Research Studies for Pfizer; received research grants from Novartis, Pfizer, Ipsen, HRA Pharma, Shire, IBSA; has been an occasional consultant for Novartis, Ipsen, Pfizer, Shire, HRA Pharma, Cortendo AB, Ferring and Italfarmaco; and has received fees and honoraria for presentations from Novartis, Shire, beyond the confines of this work. A.M.I. reports personal fees from Takeda, non-financial support from Takeda and Ipsen, and grants from Shire and Pfizer, beyond the confines of this work. A.C. has been Principal Investigator of Research Studies for Novartis, Ipsen, Pfizer, Lilly, Merck, and Novo Nordisk; consultant for Novartis, Ipsen, Pfizer, Italfarmaco and received honoraria from Novartis, Ipsen and Pfizer. The remaining authors have nothing to disclose.

**Funding sources:** The study was funded by the Ministry of Education, University and Research Grants PRIN 2017HRTZYA (to R.P.) and from University Research Grant UNINA (to M.C.D.M).

**Author contributions:** M.N. and C.P. conceived, developed, performed the study and wrote the manuscript. C.S. contributed to the analysis and interpretation of the results and to the writing of the manuscript. G.D.G., M.A.V., F.S., R.F. C.d.A, E.S., M.D.M., A.C., provided a significant expert contribution to interpretation of the results and to the writing of the manuscript. A.I. provided a significant expert contribution in the scientific revision process. R.P. supervised the analysis of data, the manuscript drafting, critically reviewed and revised it for important intellectual content. All authors read and approved the final manuscript.

Accepted manuscript

## BIBLIOGRAPHY:

1. Bell-Pedersen, D., V.M. Cassone, D.J. Earnest, S.S. Golden, P.E. Hardin, T.L. Thomas, et al., *Circadian rhythms from multiple oscillators: lessons from diverse organisms*. *Nature reviews. Genetics*, 2005. 6(7): p. 544-56.
2. Bollinger, T. and U. Schibler, *Circadian rhythms - from genes to physiology and disease*. *Swiss medical weekly*, 2014. 144: p. w13984.
3. Oster, H., E. Challet, V. Ott, E. Arvat, E.R. de Kloet, D.J. Dijk, et al., *The Functional and Clinical Significance of the 24-Hour Rhythm of Circulating Glucocorticoids*. *Endocr Rev*, 2017. 38(1): p. 3-45.
4. Refinetti, R., *Comparison of light, food, and temperature as environmental synchronizers of the circadian rhythm of activity in mice*. *The journal of physiological sciences : JPS*, 2015. 65(4): p. 359-66.
5. Buhr, E.D. and J.S. Takahashi, *Molecular components of the Mammalian circadian clock*. *Handbook of experimental pharmacology*, 2013(217): p. 3-27.
6. Partch, C.L., C.B. Green, and J.S. Takahashi, *Molecular architecture of the mammalian circadian clock*. *Trends in cell biology*, 2014. 24(2): p. 90-9.
7. Guillaumond, F., H. Dardente, V. Giguere, and N. Cermakian, *Differential control of Bmal1 circadian transcription by REV-ERB and ROR nuclear receptors*. *Journal of biological rhythms*, 2005. 20(5): p. 391-403.
8. Meng, Q.J., A. McMaster, S. Beesley, W.Q. Lu, J. Gibbs, D. Parks, et al., *Ligand modulation of REV-ERB $\alpha$  function resets the peripheral circadian clock in a phasic manner*. *Journal of cell science*, 2008. 121(Pt 21): p. 3629-35.
9. Dumbell R, Leliavski A, Matveeva O, Blaum C, Tsang AH, Oster H. Dissociation of molecular and endocrine circadian rhythms in male mice lacking bmal1 in the adrenal cortex. *Endocrinology*. 2016 DOI: 10.1210/en.2016-1330
10. Dallmann R, Touma C, Palme R, Albrecht U, Steinlechner S. Impaired daily glucocorticoid rhythm in Per1Brd mice. *J Comp Physiol A Neuroethol Sensory, Neural, Behav Physiol*. 2006 DOI: 10.1007/s00359-006-0114-9
11. Destici E, Jacobs EH, Tamanini F, Loos M, Van Der Horst GTJ, Oklejewicz M. Altered phase-relationship between peripheral oscillators and environmental time in Cry1 or Cry2 deficient mouse models for early and late chronotypes. *PLoS One*. 2013 DOI: 10.1371/journal.pone.0083602
12. Turek FW, Joshu C, Kohsaka A, Lin E, Ivanova G, McDearmon E, et al. Obesity and metabolic syndrome in circadian Clock mutant mice. *Science (80- )*. 2005 DOI: 10.1126/science.1108750

13. Oster H, Damerow S, Kiessling S, Jakubcakova V, Abraham D, Tian J, et al. The circadian rhythm of glucocorticoids is regulated by a gating mechanism residing in the adrenal cortical clock. *Cell Metab.* 2006 DOI: 10.1016/j.cmet.2006.07.002
14. Soares VR, Silva Martins C, Martinez EZ, Araujo LD, Roa SLR, Silva LR, et al. Peripheral clock system circadian abnormalities in Cushing's disease. *Chronobiol Int.* 2020 Jun;37(6):867-876. doi: 10.1080/07420528.2020.1758126.
15. Lamia, K.A., S.J. Papp, R.T. Yu, G.D. Barish, N.H. Uhlénhaut, J.W. Jonker, et al., *Cryptochromes mediate rhythmic repression of the glucocorticoid receptor.* *Nature*, 2011. 480(7378): p. 552-6.
16. Nader, N., G.P. Chrousos, and T. Kino, *Circadian rhythm transcription factor CLOCK regulates the transcriptional activity of the glucocorticoid receptor by acetylating its hinge region lysine cluster: potential physiological implications.* *FASEB journal : official publication of the Federation of American Societies for Experimental Biology*, 2009. **23**(5): p. 1572-83.
17. Charmandari E, Chrousos GP, Lambrou GI, Pavlaki A, Koide H, Ng SSM, et al. Peripheral CLOCK regulates target-tissue glucocorticoid receptor transcriptional activity in a circadian fashion in man. *PLoS One.* 2011 DOI: 10.1371/journal.pone.0025612
18. Balsalobre A, Brown SA, Marcacci L, Tronche F, Kellendonk C, Reichardt HM, et al. Resetting of circadian time in peripheral tissues by glucocorticoid signaling. *Science* (80- ). 2000 DOI: 10.1126/science.289.5488.2344
19. Gómez-Abellán P, Díez-Noguera A, Madrid JA, Luján JA, Ordoñas JM, Garaulet M. Glucocorticoids Affect 24 h Clock Genes Expression in Human Adipose Tissue Explant Cultures. *PLoS One.* 2012 DOI: 10.1371/
20. Reddy AB, Maywood ES, Karp NA, King VM, Inoue Y, Gonzalez FJ, et al. Glucocorticoid signaling synchronizes the liver circadian transcriptome. *Hepatology.* 2007 DOI: 10.1002/hep.21571
21. Segall LA, Perrin JS, Walker CD, Stewart J, Amir S. Glucocorticoid rhythms control the rhythm of expression of the clock protein, *Period2*, in oval nucleus of the bed nucleus of the stria terminalis and central nucleus of the amygdala in rats. *Neuroscience.* 2006 DOI: 10.1016/j.neuroscience.2006.03.037
22. Morgan SA, Sherlock M, Gathercole LL, Lavery GG, Lenaghan C, Bujalska IJ, et al. 11 $\beta$ -hydroxysteroid dehydrogenase type 1 regulates glucocorticoid-induced insulin resistance in skeletal muscle. *Diabetes.* 2009 DOI: 10.2337/db09-0525
23. Gathercole LL, Bujalska IJ, Stewart PM, Tomlinson JW. Glucocorticoid modulation of insulin signaling in human subcutaneous adipose tissue. *J Clin Endocrinol Metab.* 2007 DOI: 10.1210/jc.2007-1399
24. Hu Z, Wang H, In HL, Du J, Mitch WE. Endogenous glucocorticoids and impaired insulin signaling are both required to stimulate muscle wasting under pathophysiological conditions in mice. *J Clin Invest.* 2009 DOI: 10.1172/JCI38770

25. Tappy L, Randin D, Vollenweider P, Vollenweider L, Paquot N, Scherrer U, et al. Mechanisms of dexamethasone-induced insulin resistance in healthy humans. *J Clin Endocrinol Metab.* 1994 DOI: 10.1210/jcem.79.4.7962275
26. Nicod N, Giusti V, Besse C, Tappy L. Metabolic adaptations to dexamethasone-induced insulin resistance in healthy volunteers. *Obes Res.* 2003 DOI: 10.1038/oby.2003.90
27. Nielsen MF, Caumo A, Chandramouli V, Schumann WC, Cobelli C, Landau BR, et al. Impaired basal glucose effectiveness but unaltered fasting glucose release and gluconeogenesis during short-term hypercortisolemia in healthy subjects. *Am J Physiol - Endocrinol Metab.* 2004 DOI: 10.1152/ajpendo.00566.2002
28. So AYL, Bernal TU, Pillsbury ML, Yamamoto KR, Feldman BJ. Glucocorticoid regulation of the circadian clock modulates glucose homeostasis. *Proc Natl Acad Sci U S A.* 2009 DOI: 10.1073/pnas.0909733106
29. Tsang AH, Astiz M, Leinweber B, Oster H. Rodent models for the analysis of tissue clock function in metabolic rhythms research. *Front Endocrinol (Lausanne).* 2017 DOI: 10.3389/fendo.2017.00027
30. Turek FW, Joshu C, Kohsaka A, Lin E, Ivanova G, McDearmon E, et al. Obesity and metabolic syndrome in circadian Clock mutant mice. *Science (80- ).* 2005 DOI: 10.1126/science.1108750
31. Yang S, Liu A, Weidenhammer A, Cooksey RC, McClain D, Kim MK, et al. The role of mPer2 clock gene in glucocorticoid and feeding rhythms. *Endocrinology.* 2009 DOI: 10.1210/en.2008-0705
32. Kelly MA, Rees SD, Hydriem ZL, Shera AS, Bellary S, O'Hare JP, et al. Circadian gene variants and susceptibility to type 2 diabetes: A pilot study. *PLoS One.* 2012 DOI: 10.1371/journal.pone.0032670
33. Wefers J, Van Moorsel D, Hansen J, Connell NJ, Havekes B, Hoeks J, et al. Circadian misalignment induces fatty acid metabolism gene profiles and compromises insulin sensitivity in human skeletal muscle. *Proc Natl Acad Sci U S A.* 2018 DOI: 10.1073/pnas.1722295115
34. Gómez-Santos C, Gómez-Abellán P, Madrid JA, Hernández-Morante JJ, Lujan JA, Ordovas JM, et al. Circadian rhythm of clock genes in human adipose explants. *Obesity.* 2009 DOI: 10.1038/oby.2009.164
35. Harfmann BD, Schroder EA, Esser KA. Circadian rhythms, the molecular clock, and skeletal muscle. *J Biol Rhythms.* 2015 DOI: 10.1177/0748730414561638
36. Yaribeygi H, Farrokhi FR, Butler AE, Sahebkar A. Insulin resistance: Review of the underlying molecular mechanisms. *J Cell Physiol.* 2019 DOI: 10.1002/jcp.27603
37. Pivonello R, Isidori AM, De Martino MC, Newell-Price J, Biller BMK, Colao A. Complications of Cushing's syndrome: State of the art. *Lancet Diabetes Endocrinol.* 2016 DOI: 10.1016/S2213-8587(16)00086-3
38. Bornstein SR, Allolio B, Arlt W, Barthel A, Don-Wauchope A, Hammer GD, et al. Diagnosis and treatment of primary adrenal insufficiency: An endocrine society clinical practice guideline. *J Clin*

Endocrinol Metab. 2016 DOI: 10.1210/jc.2015-1710

39. Dunlop, D., Eighty-Six Cases of Addison's Disease. *British medical journal*, 1963. 2(5362): p. 887-91
40. Fleseriu M, Hashim IA, Karavitaki N, Melmed S, Murad MH, Salvatori R, et al. Hormonal replacement in hypopituitarism in adults: An endocrine society clinical practice guideline. *J Clin Endocrinol Metab*. 2016 DOI: 10.1210/jc.2016-2118
41. Bergthorsdottir R, Leonsson-Zachrisson M, Odén A, Johannsson G. Premature mortality in patients with Addison's disease: A population-based study. *J Clin Endocrinol Metab*. 2006 DOI: 10.1210/jc.2006-0076
42. Bensing S, Brandt L, Tabaroj F, Sjöberg O, Nilsson B, Ekblom A, et al. Increased death risk and altered cancer incidence pattern in patients with isolated or combined autoimmune primary adrenocortical insufficiency. *Clin Endocrinol (Oxf)*. 2008 DOI: 10.1111/j.1365-2265.2008.03340.x
43. Filipsson H, Monson JP, Koltowska-Häggström M, Mattsson A, Johannsson G. The impact of glucocorticoid replacement regimens on metabolic outcome and comorbidity in hypopituitary patients. *J Clin Endocrinol Metab*. 2006 DOI: 10.1210/jc.2006-0524
44. Danilowicz K, Bruno OD, Manavela M, Gomez RM, Barkan A. Correction of cortisol overreplacement ameliorates morbidities in patients with hypopituitarism: A pilot study. *Pituitary*. 2008 DOI: 10.1007/s11102-008-0126-2
45. Al-Shoumer KAS, Beshyah SA, Niththyananthan R, Johnston DG. Effect of glucocorticoid replacement therapy on glucose tolerance and intermediary metabolites in hypopituitary adults. *Clin Endocrinol (Oxf)*. 1995 DOI: 10.1111/j.1365-2265.1995.tb02602.x
46. Plat L, Leproult R, L'Hermite-Baleriaux M, Fery F, Mockel J, Polonsky KS, et al. Metabolic Effects of Short-Term Elevations of Plasma Cortisol Are More Pronounced in the Evening Than in the Morning *J Clin Endocrinol Metab*. 1999 DOI: 10.1210/jcem.84.9.5978
47. Isidori AM, Venneri MA, Graziadio C, Simeoli C, Fiore D, Hasenmajer V, et al. Effect of once-daily, modified-release hydrocortisone versus standard glucocorticoid therapy on metabolism and innate immunity in patients with adrenal insufficiency (DREAM): a single-blind, randomised controlled trial. *Lancet Diabetes Endocrinol*. 2018 DOI: 10.1016/S2213-8587(17)30398-4
48. Johannsson G, Nilsson AG, Bergthorsdottir R, Burman P, Dahlqvist P, Ekman B, et al. Improved cortisol exposure-time profile and outcome in patients with adrenal insufficiency: A prospective randomized trial of a novel hydrocortisone dual-release formulation. *J Clin Endocrinol Metab*. 2012 DOI: 10.1210/jc.2011-1926
49. Quinkler M, Nilsen RM, Zopf K, Ventz M, Øksnes M. Modified-release hydrocortisone decreases BMI and HbA1c in patients with primary and secondary adrenal insufficiency. *Eur J Endocrinol*. 2015 DOI: 10.1530/EJE-14-1114
50. Giordano R, Guaraldi F, Marinazzo E, Fumarola F, Rampino A, Berardelli R, et al. Improvement of

anthropometric and metabolic parameters, and quality of life following treatment with dual-release hydrocortisone in patients with Addison's disease. *Endocrine*. 2016 DOI: 10.1007/s12020-015-0681-z

51. Guarnotta V, Ciresi A, Pillitteri G, Giordano C. Improved insulin sensitivity and secretion in prediabetic patients with adrenal insufficiency on dual-release hydrocortisone treatment: a 36-month retrospective analysis. *Clin Endocrinol (Oxf)*. 2018 DOI: 10.1111/cen.13554
52. Guarnotta V, Mineo MI, Radellini S, Pizzolanti G, Giordano C. Dual-release hydrocortisone improves hepatic steatosis in patients with secondary adrenal insufficiency: A real-life study. *Ther Adv Endocrinol Metab*. 2019 DOI: 10.1177/2042018819871169
53. Guarnotta V, Di Stefano C, Santoro A, Ciresi A, Coppola A, Giordano C. Dual-release hydrocortisone vs conventional glucocorticoids in adrenal insufficiency. *Endocr Connect*. 2019 DOI: 10.1530/EC-19-0176
54. Mongioì LM, Condorelli RA, La Vignera S, Calogero AE. Dual-release hydrocortisone treatment: Glycometabolic profile and health-related quality of life. *Endocr Connect*. 2018 DOI: 10.1530/EC-17-0368
55. Frara S, Chiloiro S, Porcelli T, Giampietro A, Mazziotti G, De Marinis L, et al. Bone safety of dual-release hydrocortisone in patients with hypopituitarism. *Endocrine*. 2018 DOI: 10.1007/s12020-017-1512-1
56. Buckingham JC. Glucocorticoids: Exemplars of multi-tasking. *Br J Pharmacol*. 2006 DOI: 10.1038/sj.bjp.0706456
57. De Kloet ER, Vreugdenhil E, Oitzl MS, Joëls M. Brain corticosteroid receptor balance in health and disease. *Endocr Rev*. 1998 DOI: 10.1210/er.19.3.269
58. Yaffe D and O. Saxel, Serial passaging and differentiation of myogenic cells isolated from dystrophic mouse muscle. *Nature*, 1977. 270(5639): p. 725-7.
59. DeBruyne JP, Noton E, Lambert CM, Maywood ES, Weaver DR, Reppert SM. A Clock Shock: Mouse CLOCK Is Not Required for Circadian Oscillator Function. *Neuron*. 2006 DOI: 10.1016/j.neuron.2006.03.041
60. Landgraf D, Wang LL, Diemer T, Welsh DK. NPAS2 Compensates for Loss of CLOCK in Peripheral Circadian Oscillators. *PLoS Genet*. 2016 DOI: 10.1371/journal.pgen.1005882
61. Fu L, Lee CC. The circadian clock: Pacemaker and tumour suppressor. *Nat Rev Cancer*. 2003 DOI: 10.1038/nrc1072
62. Ye R, Selby CP, Chiou YY, Ozkan-Dagliyan I, Gaddameedhi S, Sancar A. Dual modes of CLOCK:BMAL1 inhibition mediated by Cryptochrome and period proteins in the mammalian circadian clock. *Genes Dev*. 2014 DOI: 10.1101/gad.249417.114

63. Debono M, Price JN, Ross RJ. Novel strategies for hydrocortisone replacement. *Best Pract Res Clin Endocrinol Metab.* 2009 DOI: 10.1016/j.beem.2008.09.010
64. Jiang CL, Liu L, Tasker JG. Why do we need nongenomic glucocorticoid mechanisms $\alpha$ . *Front Neuroendocrinol.* 2014 DOI: 10.1016/j.yfrne.2013.09.005
65. Barnea M, Madar Z, Froy O. Dexamethasone induces high-amplitude rhythms in preadipocytes, But hinders circadian expression in differentiated adipocytes. *Chronobiol Int.* 2013 DOI: 10.3109/07420528.2013.767824
66. Bieler J, Cannavo R, Gustafson K, Gobet C, Gatfield D, Naef F. Robust synchronization of coupled circadian and cell cycle oscillators in single mammalian cells. *Mol Syst Biol.* 2014 DOI: 10.15252/msb.20145218
67. Pivonello C, Rousaki P, Negri M, Sarnataro M, Napolitano M, Marino FZ, et al. Effects of the single and combined treatment with dopamine agonist, somatostatin analog and mTOR inhibitors in a human lung carcinoid cell line: an in vitro study. *Endocrine.* 2017 DOI: 10.1007/s12020-016-1079-2
68. Harfmann BD, Schroder EA, Esser KA. Circadian rhythms, the molecular clock, and skeletal muscle. *J Biol Rhythms.* 2015 DOI: 10.1177/0748730414561638
69. Altıntaş A, Laker RC, Garde C, Barrès R, Zierath JR. Transcriptomic and epigenomics atlas of myotubes reveals insight into the circadian control of metabolism and development. *Epigenomics.* 2020 DOI: 10.2217/epi-2019-0391
70. Balsalobre A, Damiola F, Schibler U. A serum shock induces circadian gene expression in mammalian tissue culture cells. *Cell.* 1998 DOI: 10.1016/S0092-8674(00)81199-X
71. Xiang S, Mao L, Duplessis T, Yuan L, Dauchy R, Dauchy E, et al. Oscillation of clock and clock controlled genes induced by serum shock in human breast epithelial and breast cancer cells: Regulation by melatonin. *Breast Cancer Basic Clin Res.* 2012 DOI: 10.4137/BCBCR.S9673
72. Hindmarsh, P.C. and E. Charmandari, Variation in absorption and half-life of hydrocortisone influence plasma cortisol concentrations. *Clinical endocrinology*, 2015. 82(4): p. 557-61.

**Figure 1**

**A)**

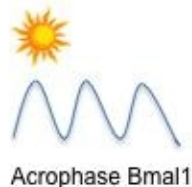
Myocytes in differentiated medium containing 2% HS

50% HS (2hr)

Serum deprivation

24hrs

**B)**



Dish 1 450 nM HC

Dish 2 650 nM HC

Dish 3 750 nM HC

Bathypphase Bmal1

Dish 1 150 nM HC

Dish 2 177 nM HC

Dish 3 300 nM HC

Figure 2

A)

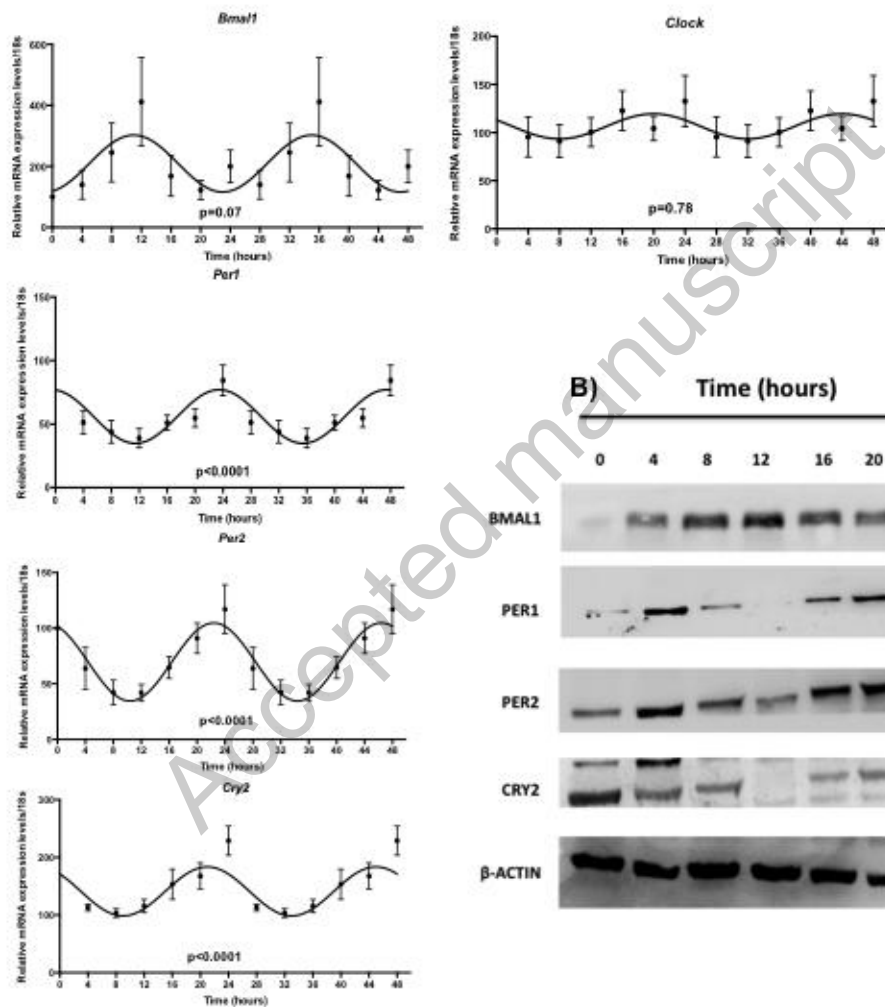


Figure 3

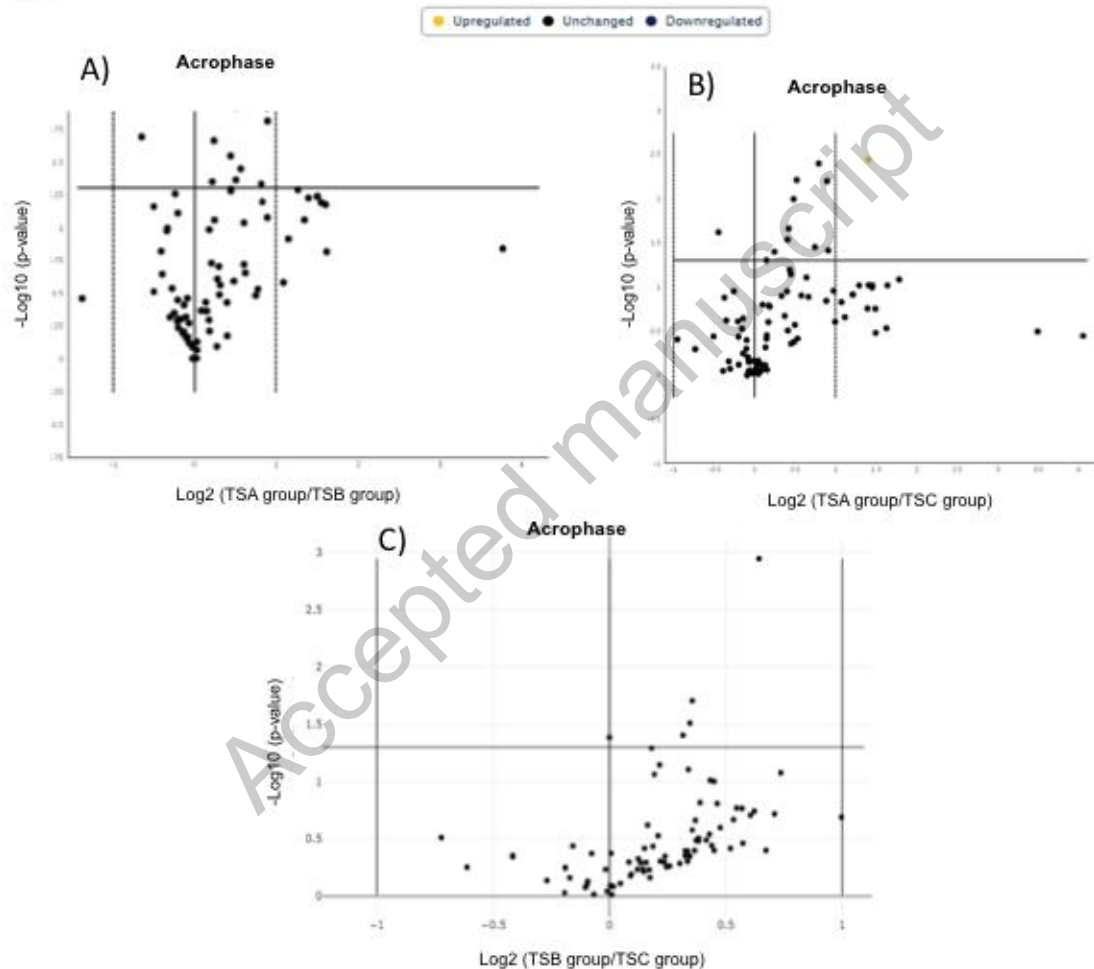


Figure 4

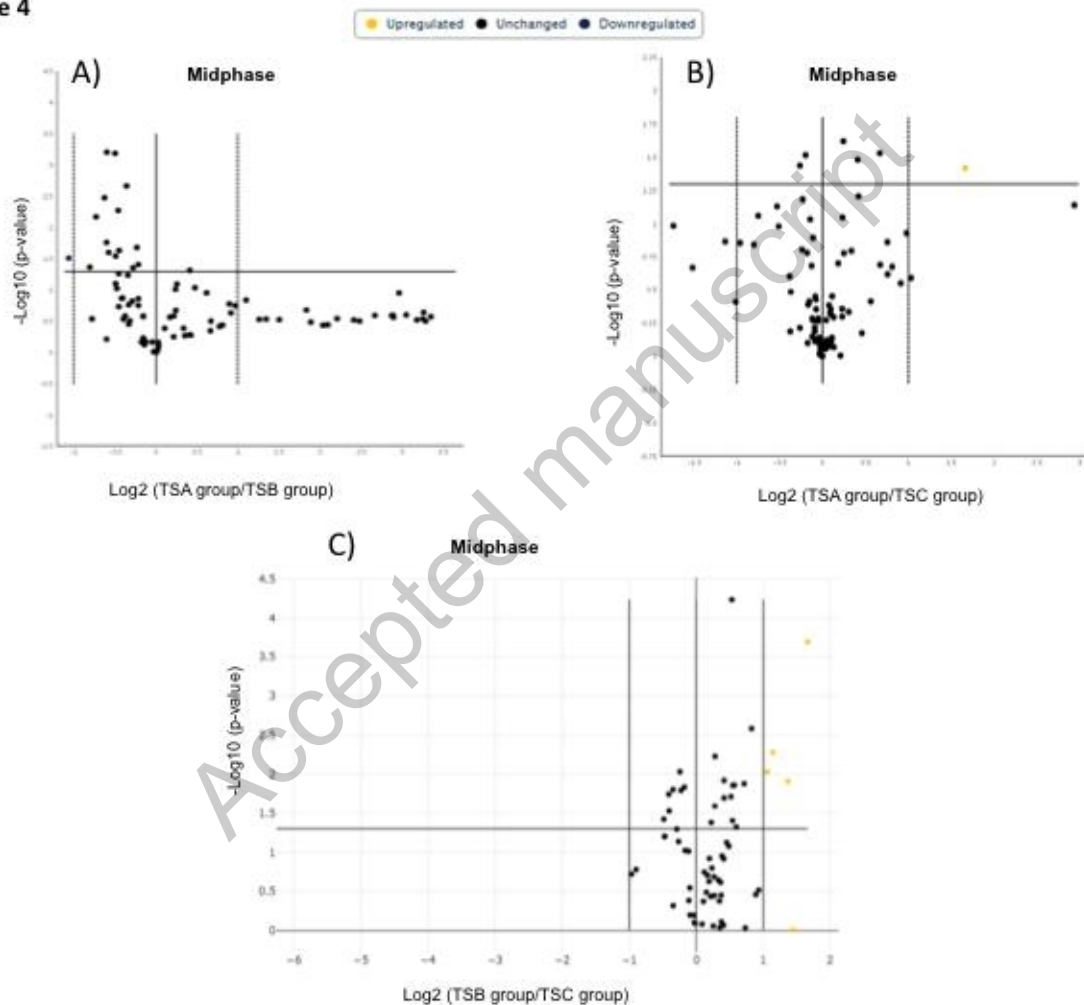


Figure 5

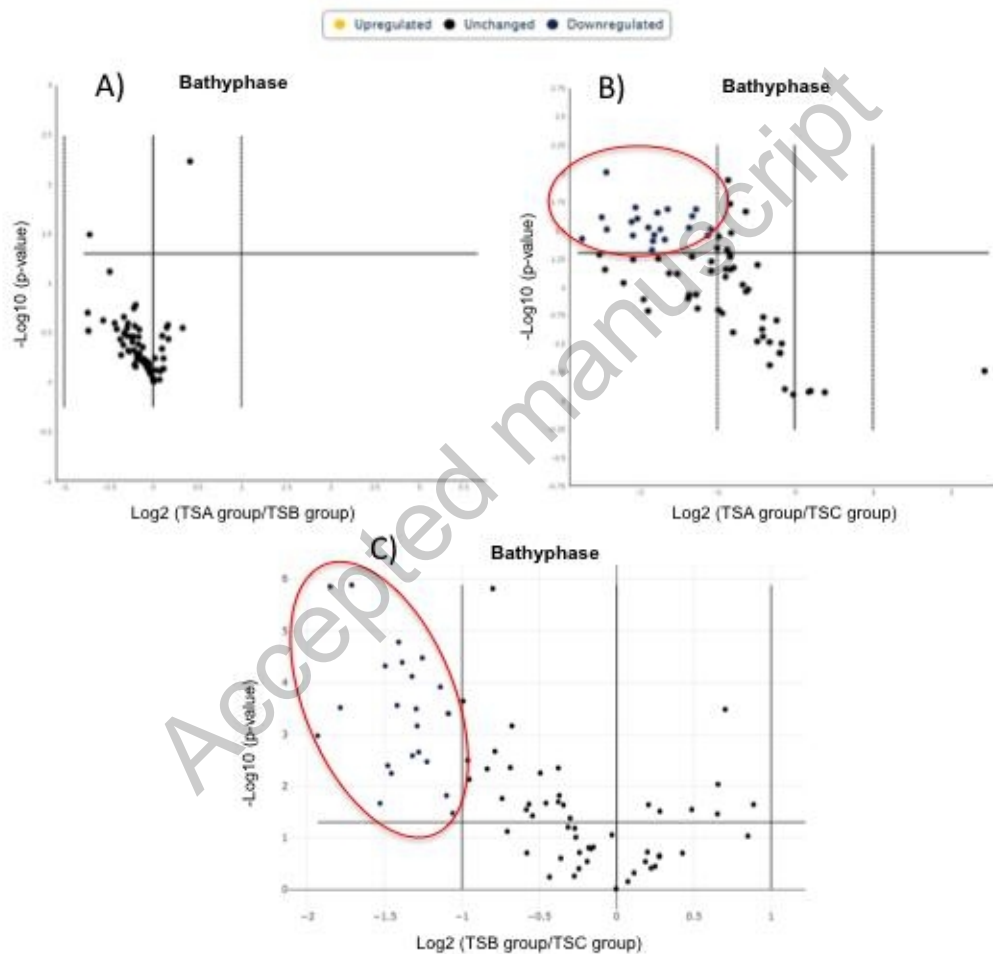


Figure 6

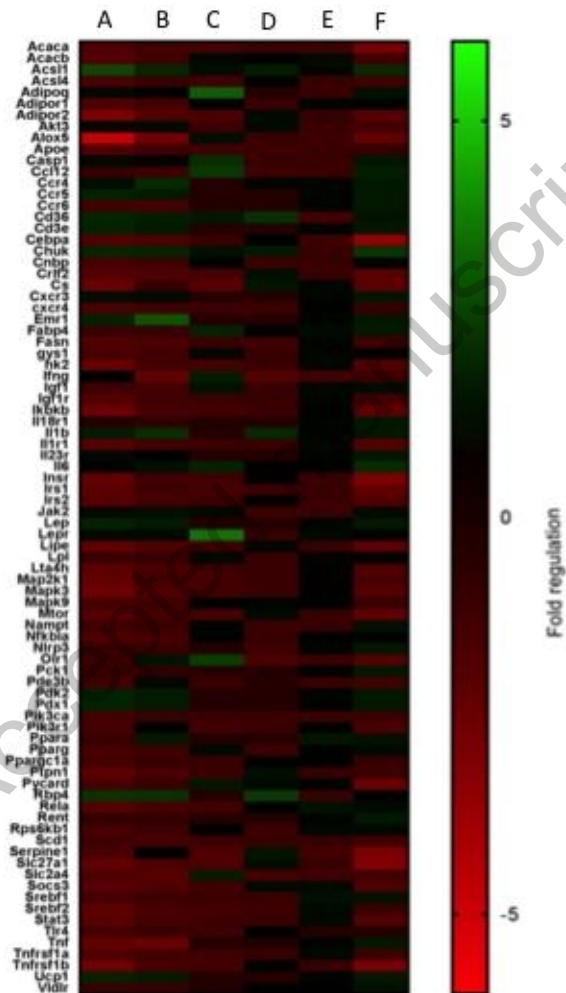
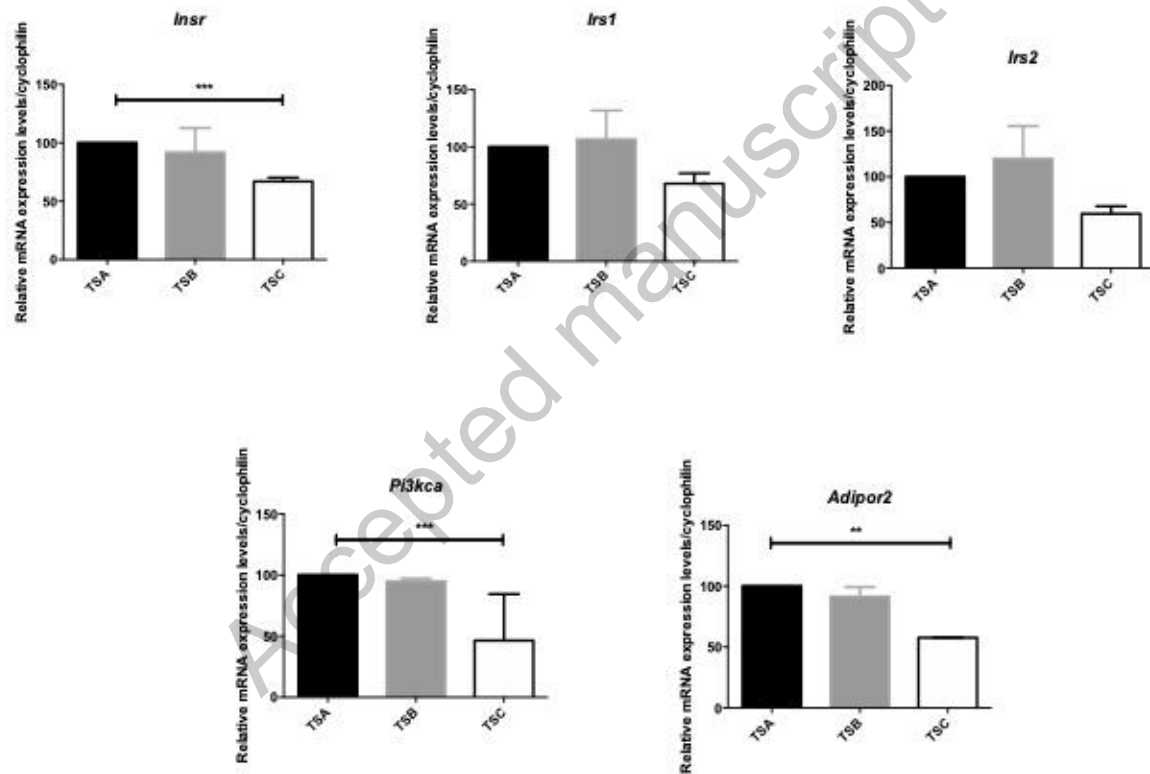


Figure 7



**Figure 8**

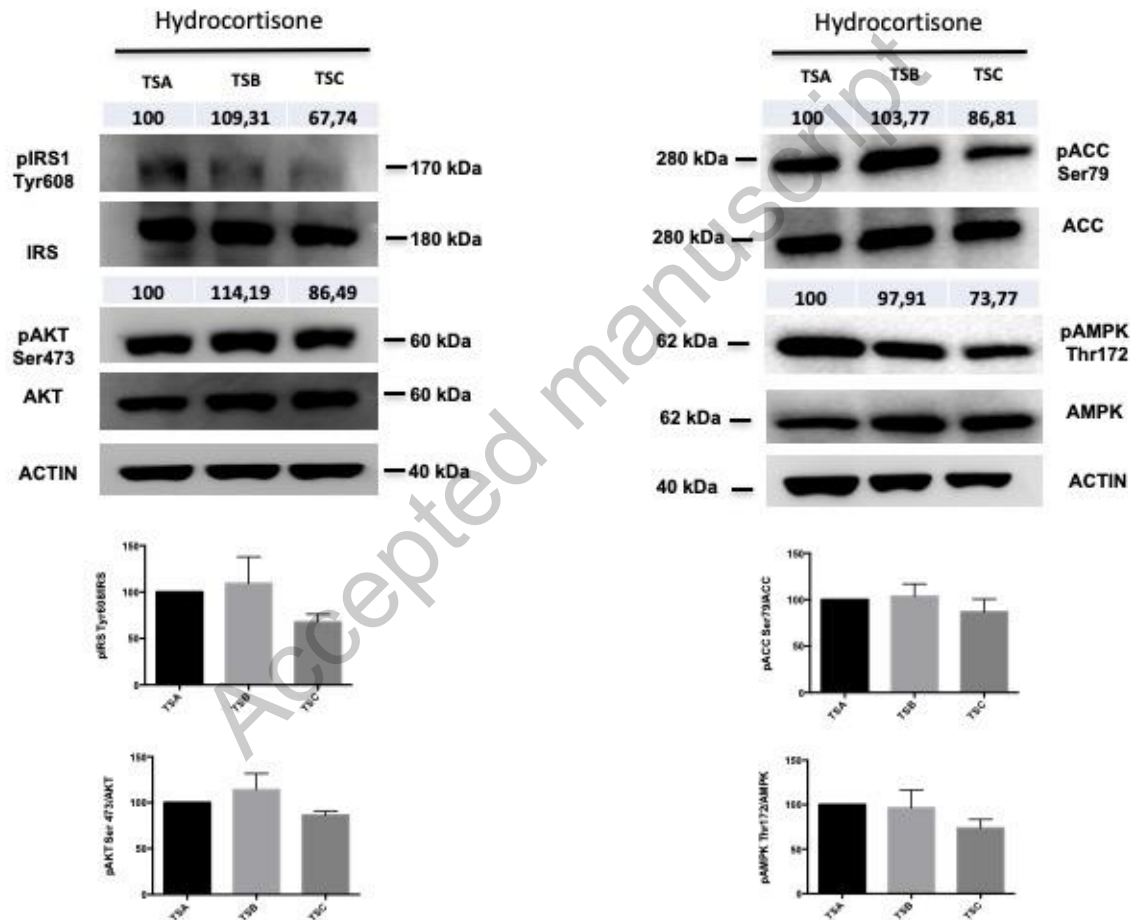
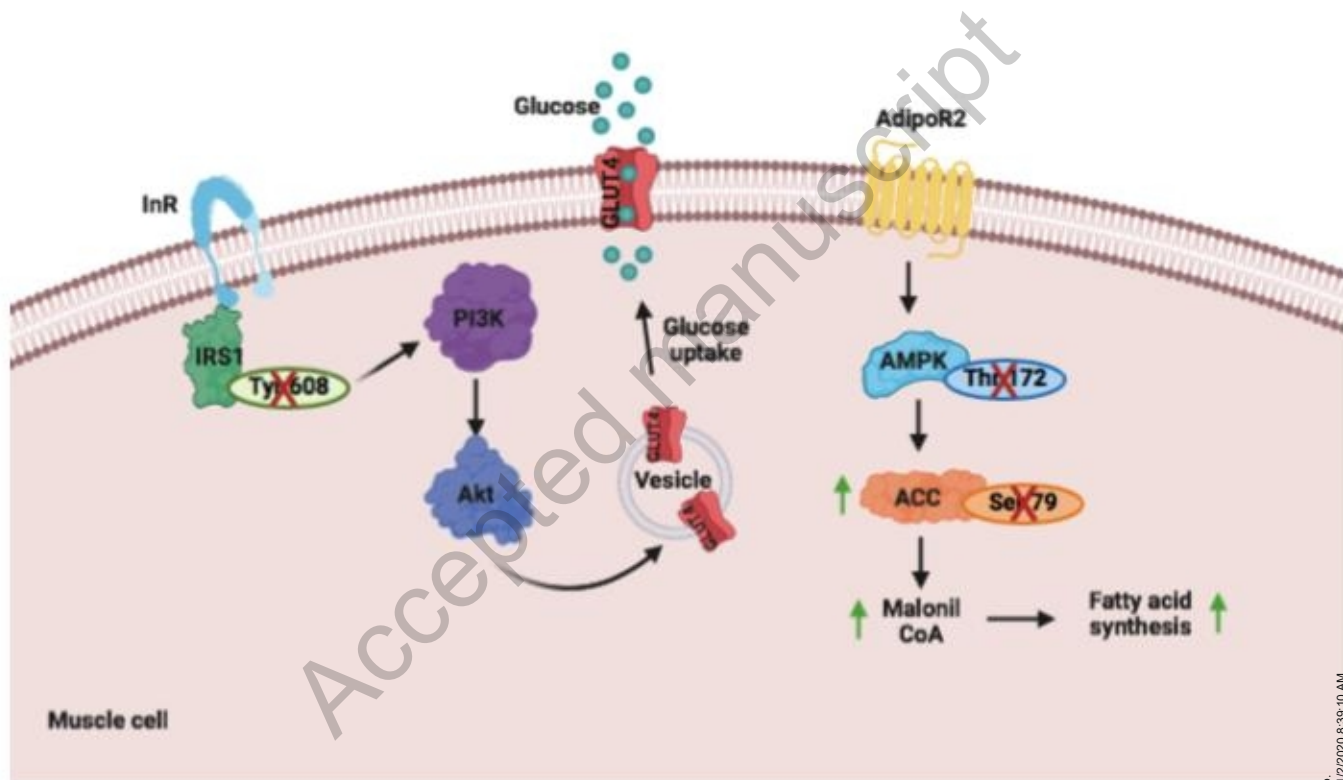


Figure 9



Accepted manuscript

<b>Time-points</b>	
<b>Hrs after starvation</b>	<b><i>Bmal1</i> gene expression</b>
12	acrophase
15	midphase
18	bathyphase

**Hydrocortisone concentrations to recapitulate *in vitro* the serum cortisol patterns observed in patients under once daily MR-HC or thrice-daily IR-HC treatments (nmol/L)**

TSA	TSB	TSC
Physiological	MR-HC	IR-HC
400	650	750
200	372	600
150	177	300

**Gene symbol**

Acaca  
Acacb  
Acsl4  
Adipor2  
Alox5  
Cebpa  
Fasn  
Ifng  
Ikbkb  
Il1r1  
Insr  
Irs1  
Irs2  
Lipe  
Lta4h  
Mapk3  
Olr1  
Plk3ca  
Socs3  
Stat3  
Tnfrsf1b

Accepted manuscript

<b>Gene name</b>	<b>Fold change</b>
Acetyl-CoA Carboxylase Alpha	-5.37
Acetyl-CoA Carboxylase Beta	-2.49
Long-chain-fatty-acid—CoA ligase 4	-2.57
Adipokine receptor 2	-3.70
Arachidonate 5- Lipoxygenase	-4.29
CCAAT/enhancer binding protein alpha	-6.68
Fatty acid synthase	-2.42
Interferon gamma	-2.18
Inhibitor of nuclear factor kappa B kinase subunit beta	-4.25
Interleukin 1 receptor	-3.59
Insulin receptor	-5.60
Insulin receptor substrate 1	-4.15
Insulin receptor substrate 2	-3.32
Lipase E	-4.08
Leukotriene A4 Hydroxylase	-3.11
Mitogen-Activated Protein Kinase 3	-3.55
Oxidized low density lipoprotein receptor 1	-3.51
Phosphatidylinositol-4,5-bisphosphate 3-kinase catalytic subunit alpha	-2.11
Suppressor Of Cytokine Signaling 3	-3.19
Signal transducer and activator of transcription 3	-3.42
Tumor necrosis factor receptor superfamily, member 1b	-5.35

**p-value**

0.009718  
0.023602  
0.029905  
0.029810  
0.026506  
0.037441  
0.020579  
0.034901  
0.034995  
0.046924  
0.024156  
0.019819  
0.030917  
0.024886  
0.020585  
0.039112  
0.034575  
0.030844  
0.038021  
0.022028  
0.030947

Accepted manuscript

**Gene symbol**

Acaca  
Adipor2  
Alox5  
Cebpa  
Crlf2  
Cs  
Hk2  
Ikbkb  
Il1r1  
Insr  
Irs1  
Irs2  
Lipe  
Lta4h  
Mapk3  
Mtor  
Olr1  
Pycard  
Serpine1  
Slc27a1  
Socs3

Accepted manuscript

<b>Gene name</b>	<b>Fold change</b>
Acetyl-CoA Carboxylase Alpha	-2.75
Adipokine receptor 2	-2.50
Arachidonate 5- Lipoxygenase	-2.09
CCAAT/enhancer binding protein alpha	-3.82
Cytokine Receptor Like Factor 2	-2.20
Citrate synthase	-2.68
Hexokinase 2	-2.39
Inhibitor of nuclear factor kappa B kinase subunit beta	-2.82
Interleukin 1 receptor	-2.50
Insulin receptor	-3.28
Insulin receptor substrate 1	-2.45
Insulin receptor substrate 2	-2.12
Lipase E	-2.79
Leukotriene A4 Hydroxylase	-2.13
Mitogen-Activated Protein Kinase 3	-2.43
mammalian target of Rapamycin	-2.62
Oxidized low density lipoprotein receptor 1	-2.14
Phosphatidylinositol-4,5-bisphosphate 3-kinase catalytic subunit alpha	-2.89
Serine proteinase inhibitor 1	-2.34
Solute Carrier Family 27 Member 1	-3.61
Suppressor Of Cytokine Signaling 3	-2.46

Accepted manuscript

**p-value**

0.005650  
0.002580  
0.033591  
0.001066  
0.000122  
0.000276  
0.000034  
0.000048  
0.000076  
0.000001  
0.000686  
0.000400  
0.004016  
0.000395  
0.002200  
0.000041  
0.015128  
0.021533  
0.003379  
0.000001  
0.000324

Accepted manuscript

Accepted manuscript

**TaqMan<sup>®</sup> Assay ID**

Mm00500226\_m1

Mm00455950\_m1

Mm00501813\_m1

Mm00478113\_m1

Mm01331542\_m1

Mm04277571\_s1

<b>Gene</b>	<b>Dye</b>
Bmal1	FAM-MGB
Clock	FAM-MGB
Per1	FAM-MGB
Per2	FAM-MGB
Cry2	FAM-MGB
18S	FAM-MGB

Accepted manuscript

Accepted manuscript

<b>SybrGreen®</b>	<b>Accession number or primers</b>	<b>Gene</b>
	NM_010568	INSR
	NM_010570	IRS1
	NM_001081212	IRS2
	NM_008839	PI3KCA
	NM_197985	ADIPOR2
	Fwd: 5' GCAGACAAAGTTCCAAAGACA 3'	
	Rvs: 5' ACCCTGGCACATGAATCC 3'	Ciclophylin A

Accepted manuscript

Figure 1S

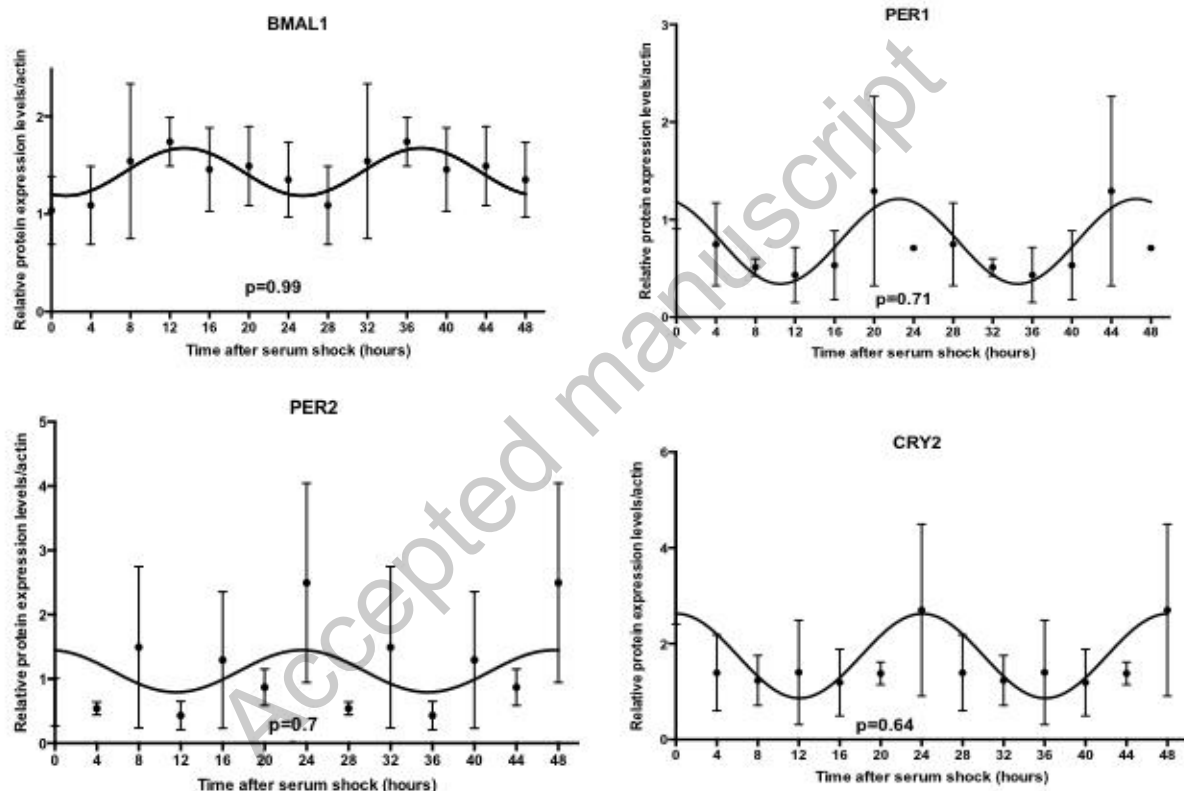


Figure 1S: Double plotted graphs illustrating the temporal rhythm organization of BMAL1, CLOCK, PER1, PER2 and CRY2 proteins in synchronized C2C12 cell line during 24hrs. Values represent the mean  $\pm$  SEM of two or three independent experiments. P values depicted in each graphs were calculated by ANOVA

Table 2S

	Gene symbol	Gene name				
	<i>Acaca</i>	Coenzyme A carboxylase alpha				
	<i>Acacb</i>	Coenzyme A carboxylase beta				
	<i>Acs1</i>	Acyl-CoA synthetase long-chain family member 1				
	<i>Acs4</i>	Acyl-CoA synthetase long-chain family member 4 Adiponectin, C1Q and collagen domain containing Adiponectin receptor 1				
	<i>Adipoq</i>	Adiponectin, C1Q and collagen domain containing Adiponectin receptor 1				
	<i>Adipor1</i>	Adiponectin receptor 1				
	<i>Adipor2</i>	Adiponectin receptor 2				
	<i>Akt3</i>	Thymoma viral proto-oncogene 3				
	<i>Alox5</i>	Arachidonate 5-lipoxygenase				
	<i>ApoE</i>	Apolipoprotein E				
	<i>Casp1</i>	Caspase 1				
	<i>Ccl12</i>	Chemokine (C-C motif) ligand 12				
	<i>Ccr4</i>	Chemokine (C-C motif) receptor 4				
	<i>Ccr5</i>	Chemokine (C-C motif) receptor 5				
	<i>Ccr6</i>	Chemokine (C-C motif) receptor 6				
	<i>Cd36</i>	CD36 antigen				
	<i>Cd3e</i>	CD3 antigen, epsilon polypeptide				
	<i>Cebpa</i>	CCAAT/enhancer binding protein (C/EBP), alpha				

--	--	--	--	--	--	--

Accepted manuscript